AD-A165 992 MICROSTRUCTURE/PROPERTY RELATIONSHIPS FOR CARBON FIBER REINFORCED ALUMINU.. (U) MASSACHUSETTS INST OF TECH CAMBRIDGE MATERIALS PROCESSING CEN.. R G DIXON ET AL. 1/2

UNCLASSIFIED 25 JUL 85 N00014-83-K-0677 F/G 11/6 NL

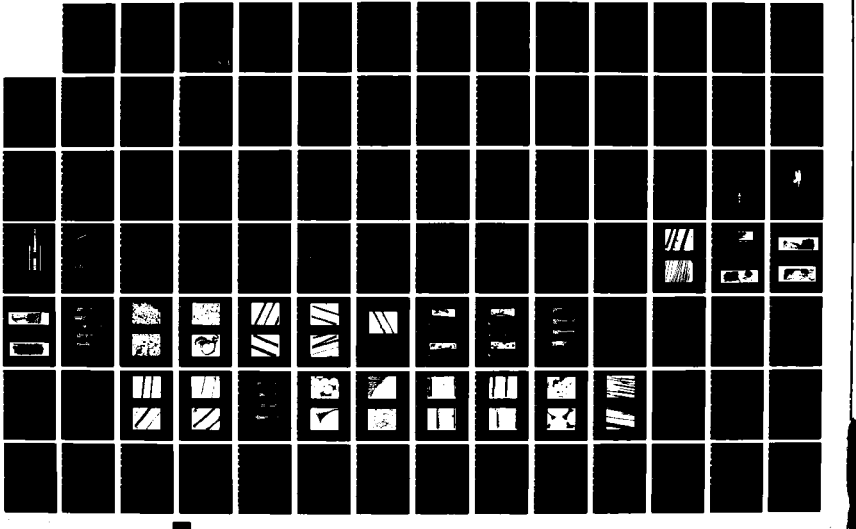

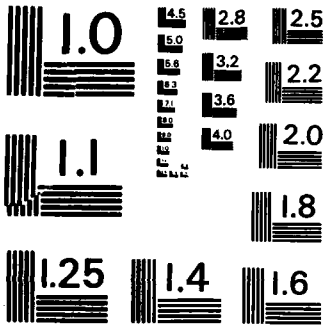

MICROSTRUCTURE/PROPERTY RELATIONSHIPS FOR CARBON FIBER REINFORCED ALUMINUM ALLOY

by

R.G. DIXON

J.A. CORNIE

M.C. FLEMINGS

MASSACHUSETTS INSTITUTE OF TECHNOLOGY
Cambridge, Massachusetts 02139

MICROSTRUCTURE/PROPERTY RELATIONSHIPS FOR CARBON FIBER REINFORCED ALUMINUM ALLOYS

by

R.G. DIXON

J.A. CORNIE

M.C. FLEMINGS

MASSACHUSETTS INSTITUTE OF TECHNOLOGY
Cambridge, Massachusetts 02139

July 25 1985

Final Technical Report
Contract Number N00014-83-K-0677

Approved for Public Release; Distribution Unlimited

Prepared for

OFFICE OF NAVAL RESEARCH
Arlington, Virginia 22217

MICROSTRUCTURE/PROPERTY RELATIONSHIPS FOR CARBON FIBER REINFORCED ALUMINUM ALLOYS

BY

R. G. DIXON
J. A. CORNIE
M. C. FLEMINGS

ABSTRACT

Graphite fibers with various coatings were tested for strength. Longitudinal composites were produced from the coated fibers using pure aluminum as the matrix by pressure casting. The strength and microstructure of the composites was evaluated. Longitudinal and transverse composites were also produced using uncoated graphite fibers with various alloy matrices and their strength and microstructure evaluated. The coated fibers were leached from the pure aluminum matrix and examined. The uncoated graphite fibers were leached from the alloy matrices and tested for strength.

The coated fibers were not found to be stronger than the uncoated fibers, nor were they effective in increasing composite strengths. Composites produced from uncoated fibers and alloy matrices were quite strong longitudinally with strengths of up to 93 percent of rule of mixtures strength. The same material, when tested in the transverse direction exhibited low strengths, with the failure being interfacial.

TABLE OF CONTENTS

LIST OF FIGURES

LIST OF TABLES

This page intentionally left blank.

INTRODUCTION AND LITERATURE SURVEY

Perhaps the primary motivating factor for the development of ceramic fiber reinforced metals was the prospect of achieving strengths greater than polymeric matrices afforded. Additionally, some other significantly superior property enhancements could be realized by the use of a metallic matrix with the high strength, high modulus graphite fibers. Perhaps most notably are the potential for high temperature applications, good electrical and thermal conductivity, low cost, good fatigue and toughness characteristics, and ease of machining and fabrication. The high temperature capability of these composites allow for their use in temperature regimes well above that of polymeric matrix composites.

Obviously the most significant constituent in the composite from a strength viewpoint is the fiber. In general, materials contain many intrinsic defects which act in various ways to lower their strengths as compared to their theoretical strengths. Kelly suggests that the theoretical strength of many materials may be estimated to be about ten percent of the modulus [1]. In reality, observed strengths are much lower. Thus, from this notion of defect structures, one may intuitively speculate that smaller specimens of like geometry would be stronger for a

given material. In fact, Griffith showed this to be the case for brittle materials in the early 1920's [2,3].

Graphite has the highest modulus and theoretical strength of all the elements and in fact for most materials known to man [4,5]. This strength is realized, however, only in the two orthogonal directions of the basal planes and is relatively weak in tension normal to these basal planes [6]. It follows logically, then, that if one could make a very fine fiber of highly oriented graphite, its strength would be a function of its diameter and degree of orientation and would be, in general, quite strong. This is, in fact, the case and graphite fibers have been produced possessing strengths of 750 Ksi and modulus values of 120 Msi (although these strength and modulus values are not for the same fiber) [7]. These considerations coupled with the fact that graphite has a maximum use temperature of around 4000 degrees Fahrenheit [8], make graphite fibers ideal candidates as reinforcing elements in composites.

Metallic matrices in composites afford many advantages over polymeric matrices and as such have been considered for a number of years for many applications. Aluminum in particular has gained a wide acceptance as a matrix material as it affords many advantages over other candidate metallic matrices. Graphite reinforced aluminum composites have a very high strength to weight ratio and are thus

considered for use where weight savings have considerable payoffs such as in the aerospace industry and, to a lesser extent, the automotive industry. In addition to good specific strengths, aluminum alloys readily with many elements and its strength can be increased dramatically with relatively small alloy additions. Excellent electrical and thermal conductivity to weight ratios can be realized through the use of graphite/aluminum composites. Obviously high temperature service is an important concern and alumimum affords a great improvement over polymeric matrices in this arena. Some disadvantages, however, do exist for aluminum as a matrix material. Perhaps the most serious is the chemical reactivity of aluminum. Even at room temperature aluminum is a very reactive element and at temperatures necessary for composite fabrication (750 degrees Celsius), it is even more reactive. As temperatures required for fiber degradation (i.e. melting, sublimation, etc.) are very large compared to composite fabrication temperatures, thermal damage to the fiber is minimal if existant at all in composite production. Recognizing the fact that the mechanism for fiber degradation is likely to be chemical rather than thermal in nature, the high reactivity of aluminum can be a serious concern.

Another problem in the production of graphite

reinforced aluminum composites is the wetability of graphite by aluminum. The basal planes of an oriented graphite fiber are generally at its surface and these planes provide little in the way of bonding sites [9]. Thus, most metals do not wet the surface of graphite with aluminum being no exception. At the melting point of aluminum, the contact angle between graphite and the liquid aluminum is larger than 90 degrees and thus wetting is not spontaneous [10]. The aluminum, then, must be forced between the fibers under pressure to assure intimate contact between fibers and metal and thus adequate load transfer from matrix to fiber in the final composite. At temperatures above 1000 degrees Celsius, however, aluminum does wet graphite but there is also a reaction at this high temperature to form aluminum carbide (Al_4C_3) which can have very serious effects on the integrity of the fiber [11]. To overcome this problem of wetting, various coatings have been considered and subsequently employed on the fiber surface. In addition to promoting wetting, the ideal coating for a graphite fiber in an aliminum matrix should provide for: (1) chemical compatibility between fiber and matrix, (2) a diffusion barrier preventing excessive formation of reaction products at the interface, (3) a state of bonding and interface microstructure sufficient to transfer load between matrix and fiber, and (4) stability at high temperatures that may be encountered during

fabrication or service. The fiber-matrix interface, as discussed herein, is an interfacial zone rather than a sharp mathematical interface. This zone between fiber and matrix may be from a few nanometers to a few microns in thickness. Additionally, this zone may have a variable chemical composition and a gradient microstructure that reflects and influences the properties of the composite as a whole. Thus, the interface may be considered to be a reaction zone, coating(s), or a combination of the two. Further, the interface may contain more than one layer within the zone, each internal boundary being characterized by a specific interfacial energy. Perhaps the interface is the most important part of a composite insofar as mechanical properties are concerned. Surprisingly, little more has been learned about the contribution of the interface to mechanical properties since 1974 with the publication of Metcalf's Interfaces in Composites [12].

One source of the inadequate performance of metal matrix composites has been the loss of strength due to reaction layers between the fibers and the metal matrix. [13,14,15]. Metcalf and Klein were the first to systematically study the effects of reaction zones on the mechanical properties of uniaxially reinforced boron/titanium composites [16]. Metcalf noted that in well bonded composites with the reaction zones forming at the

elevated temperatures of fabrication or service, the composite properties were essentially unaffected until a critical zone thickness had been exceeded. The tensile strength of the composite then degraded in proportion to the reaction zone thickness. The same effect was reported by Freidrich and Pompe for stainless steel wires in an aluminum matrix [17] and by Shorshorov for silicon carbide coated boron fibers [18]. Shorshorov's study showed that the strength of the composite was inversely proportional to the silicon carbide coating thickness. Cornie, et al., documented the effect of a hafnium carbide diffusion barrier coating deposited on the surface of a silicon carbide fiber [19]. This study also confirmed the aforementioned conclusions, however upon examination of the data and calculation of the fracture toughness of the filament it was found to have a value nearly three times greater than bulk silicon carbide. Cornie attributed this increase to compliance and delamination at the carbon-rich surface zone on the silicon carbide fiber.

Traditionally, the fiber-matrix interfacial bond strength was thought to be the governing factor in composite strength. That is, strong bonding produces strong composites [20]. At about the same time as Cornie's experimental work, however, Ochiai and Murakami, in 1979, advanced a theory suggesting that this may not necessarily be the case [21]. They showed that a weak interface may,

in fact, lead to improved composite properties in some materials by a delamination at the interface, thereby blunting and subsequently arresting approaching cracks. Cornie's results appear to agree, at least in principle , with Ochai and Murakami's theory and composites produced from Cornie's fibers proved to be quite strong longitudinally.

Interfacial reaction between graphite fibers and aluminum matrices are well documented. Blankenburgs determined that aluminum carbide (Al_4C_3) is produced at the interface and the growth of the carbide takes primarily in the aluminum matrix. During the latter stages of growth, however, the carbide penetrates the fiber surface thereby introducing surface flaws in the fiber [22]. Blankenburgs also determined that growth of the carbide begins as fine platelets with the c-axis of the hexagonal carbide lattice perpendicular to the platelets. These platelets have a random orientation with respect to the fiber and an irregular layer results on the fiber surface. These platelets become thicker as growth continues until they coalesce in latter stages. Although the reaction is very temperature dependent, the reaction was not observed to be very extensive at temperatures up to 645 degrees Celsius. Several studies have been performed on the effect of the reaction products, in the graphite reinforced aluminum

system, on composite properties but the conclusions are somewhat contradictory. Harrigan reports that even long time exposure at high temperatures does not significantly change the interface and the strength of the composite is not degraded [23]. Pepper et al. report that aluminum carbide formation leads to lower composite properties [24]. Jackson reported that exposure for one week at 500 degrees Celsius showed no noticible loss in strength while composites exposed at temperatures above 600 degrees Celsius for one day exhibited much lower strengths [25]. Similarly, Kahn showed that up to 500 degrees Celsius little degradation occured while above 500 degrees Celsius, the degradation was a very strong function of temperature [26].

The objectives of this study are two fold. The first area of interest is coated fibers. Various coatings will be examined and their effectiveness in improving composite strength evaluated. The coating materials and the thickness of the coatings have been prescribed only by intuition as no data currently exist in this area to guide the decision. Only now are researchers thoughts turning to a micromechanical model of the interface. Such modelling is greatly needed to specify coating materials that will achieve the desired result and a truly tailored composite be designed. A 'zeroth' order analysis is presented in the appendix [27]. Secondly, the effect of reaction product

formation during composite fabrication on fiber and composite strengths will be evaluated for several alloy systems.

PLAN OF WORK

A. EVALUATION AND EXAMINATION OF COMPOSITES WITH VARYING FIBERS

1. Test as recieved fibers coated fibers and compare strength with uncoated fibers.
2. Produce composites from coated fibers and compare strength with composites produced from uncoated fibers each with pure aluminum matrices.
3. Test composites.
4. Examine fracture surfaces and microstructure of composites.
5. Leach fibers from produced composites.
6. Examine leached fiber surfaces.

B. EVALUATION AND EXAMINATION OF COMPOSITES WITH VARYING MATRICES

1. Produce composites from commercially available graphite fibers with matrices of Al-Li, Al-Mg, Al-Si, and Al-Cu alloys.
2. Test composites for strength.
3. Examine composite microstructures for thickness of reaction zone.
4. Leach fibers from produced composites.
5. Test fibers for strength.
6. Examine fiber surfaces.

MATERIALS

The crucibles and molds used in the production of the composites are high density graphite obtained from Union Graphite of Bridgewater, MA, and from Micromechanics of Newburyport, MA.

All coated fibers were provided by Cordec Corporation of Lorton, Virginia. The fibers obtained were Union Carbide Thornel P-55 10 micron diameter graphite coated with: (1) carbon; (2) silicon; (3) silicon and aluminum; and (4) carbon, silicon and aluminum. The carbon coating and the silicon coating are each reported by the supplier to be approximately 250 angstroms thick. The aluminum was reported to be deposited to a depth of one micron. The coatings were deposited by the supplier onto spread tows of the fibers by ion plating.

All uncoated fibers were Union Carbide Thornel P-55 10 micron graphite. These fibers were supplied as a 2000 fiber tow wound around a cardboard tube.

The alloys used in this study were: (1) pure aluminum, (2) Al2.3Li, (3) Al7.8Mg, (4) Alloy 357 (Al-7Si0.5Mg), and (5) Al4.5Cu. All alloy compositions were confirmed by chemical analysis.

EQUIPMENT

All fibers tested during the course of this study were performed through the use of a card testing method. The fibers were mounted on the cardboard card (Figure 1). The cards were made to order by Globe Rubber Company of Rockland , MA. The card containing the fiber was placed in an apparatus previously designed at M.I.T. and modified by the author (Figure 2, Figure 3). The apparatus consists of an inner Teflon coated stainless steel cylinder sliding in an outer stainless steel cylinder. Attached to both inner and outer cylinders are tool steel indexing pins that correspond to mounting holes in the testing card. The apparatus is mounted in an Instron Model 1122 screw type testing mechanical testing machine. The larger outer cylinder is connected to the base of the Instron machine through the use of a rigid steel pin. The upper cylinder is connected to the Instron crosshead via a universal joint and steel pins. All fiber tests were performed using a 2000 gram load cell.

The apparatus for producing all composites consists of a graphite crucible within an induction heating coil. Pressure is applied and measured using an Instron Model TTB Universal screw type mechanical testing machine.

Contained within the induction heating coil is a large Pyrex glass tube with a 0.25 inch thick grphite susceptor

tube inside (Figure 4). The glass tube is protected from extreme heat by a thin layer of insulating material between the susceptor and the glass. When high frequency alternating electric current is applied to the coil, the graphite tube is heated by induction heating. The graphite crucible containing the composite mold is contained within the graphite susceptor and is heated by radiation from the susceptor. The Pyrex tube is sealed on the top and bottom by rubber covered, water cooled steel plates with feed throughs for thermocouples, plunger, argon, and vacuum. After sealing the Pyrex tube, a vacuum is drawn using a mechanical vacuum pump, and the tube evacuated. Two type K thermocouples, connected to an Omega Model 2176A digital thermometer, are used to measure temperatures in the crucible. A capacitive low pass filter is used to remove the interference signal induced in the thermocouples by the radio frequency (RF) of the generator.

The Lepel 12.5 KVA induction unit is used to heat the crucible and operated under the following conditions:9 Khz, 70 percent power.

When the metal in the crucible is molten, it is forced into the mold containing the fibers using the crosshead motion of the Instron machine. The load applied is measured with a 10,000 pound load cell and a plot of load versus displacement (time) is generated on the Instron chart recorder.

Scanning electron micrographs were produced using a Cambridge Stereoscan Mark IIA scanning electron microscope and an AMR model 1000A scanning electron microscope.

EXPERIMENTAL PROCEDURE

Fiber Testing

Fiber testing was performed in accordance with ASTM standard D3379 [28]. The black fibers were placed on a white work surface and cut into 2 inch lengths. A single filament was randomly chosen from the fiber bundle. The specimen was centered on the testing card (figure 1) and one end taped to the card. The filament was then lightly stretched across the card and the opposite end of the fiber taped to the card. A small amount of Duco cement was placed on the fiber at the inner edge of the testing card with a hypodermic syringe and blunted needle.

After mounting the fiber, the card containing the fiber is inserted into the test fixture (figure 2). The edges of the card are then cut and the Instron crosshead engaged. The crosshead velocity was 10 millimeters per minute. After fiber fracture, the ends of the cards were saved to measure the fiber cross sectional area. The portion of the fiber between the fiber and the tape was photographed at 600x and the measurement of fiber diameter was obtained by measuring the photographic image. Fifteen such photographs were taken of randomly selected fibers to determine average specimen area. From load and cross

sectional area measurements, the strength of the fibers was then determined.

Composite Production

The production of the longitudinal composites was acomplished by laying the fibers longitudinally in channels machined in high density graphite (figure 5). The appropriate number of fibers was determined based upon the manufacturers report of 2000 fibers per bundle. The transverse specimens were prepared by taking the appropriate number of fibers and forming a prepreg by the light application of polymethylmethacrylate (PMMA). This prepreg was then cut into appropriate lengths to fit transversely in the mold as shown in figure 6. A three piece mold was used as shown in figure 7 allowing both a longitudinal and a transverse specimen to be cast simultaneously.

The die containing the fibers was then placed into a crucible made from high density graphite (figure 4). The crucible is then sealed on top and bottow by steel plugs separated by a wool of Saffil, used here as a material to entrap and freeze off any metal that might leak past the mold. The charge of metal was placed directly on top of the fiber containing mold. A steel plunger was then inserted into the top of the crucible and the entire

crucible assembly placed inside the graphite susceptor, with the steel plunger fed through a port in the top cover plate. The graphite susceptor was contained within a large Pyrex outer tube so that a vacuum may be drawn on the system after sealing the top and the bottom of the Pyrex tube. The top and bottom plates of the assembly were water cooled. Two type K thermocouples were inserted through ports in the top cover plate and into holes in the crucible. One thermocouple was used to measure the metal charge temperature while the other was in the vicinity of the fiber containing mold.

After sealing the system, a dynamic vacuum was drawn and maintained on the system with a mechanical vacuum pump. A mercury manometer was used to monitor the vacuum. When a vacuum of 755 mm Hg or better had been achieved, the induction coils were energized. Figure 9 shows a typical heating curve. When the temperature of the mold was about 40 degrees Celsius above the liquidus of the alloy, the induction unit was turned off and the Instron crosshead was engaged producing a downward velocity on the steel plunger of 0.5 inches per minute thus forcing the metal into the mold. The infiltration time was generally 3.5 to 4 minutes. After this time the crosshead was stopped but pressure was maintained on the system until the temperature was below the solidus temperature of the alloy. All

pressure was then removed and the system allowed to cool while still maintaining vacuum. Figure 10 shows a typical cooling curve. When the mold had cooled to a temperature of less than 200 degrees Celsius, the vacum was released and the crucible removed. The mold was driven out of the crucible through the use of a hammer and punch. The mold was then opened and the specimen removed.

Composite Testing

Composites were tested in accordance with ASTM standard D3552 [28]. The specimens were cut into one inch lengths for testing. Figure 8 shows the general design of the composite specimens. Aluminum tabs 0.030 inch thick with a 45 degree taper from tab to specimen were epoxied to the composite specimens. The surface of both the tab and the specimen were prepared by a light sanding with 3/0 emery paper and cleaning with an alcohol swab. The tapered tabs provided for a more gradual transfer of load from testing machine to specimen and minimized the stress concentration induced by the large section change of an untabbed specimen. After allowing the epoxy to cure for 24 hours at room temperature, and measuring the specimen cross section, the specimens were tested using an Instron model 1122 screw type mechanical testing machine outfitted with wedge shaped grips and a 1000 pound load cell. The

crosshead velocity was 10 millimeters per minute. From the load and cross sectional area, strength data were generated.

Fiber Leaching

Fibers were leached from the composites by using a solution of 40 grams of NaOH in one liter of water. The composites were immersed in the room temperature solution until all the aluminum had been dissolved (approximately two hours). The fibers were washed with 500 ml of water followed by 25 ml of absolute ethanol.

Metallurgical Specimen Preparation

In samples where interfacial reaction products were to be observed, metallurgical specimens were prepared without the use of water. Grinding and polishing was accomplished through the use of absolute ethanol and no etchant used. A suspension of alumina in absolute ethanol was used for final polishing. Conventional metallography was performed on all remaining specimens. The etchant used for all cases was Keller's etch (2 ml HF, 3 ml HCl, 5 ml HNO_3, 190 ml water) [29].

RESULTS AND DISCUSSION

Tensile Tests of Coated Fibers

Figure 11 shows the strength distributions for the as recieved uncoated 10 micron P55 baseline fiber. The mean strength, for 16 samples, was found to be 274 ksi. Figure 12 shows the distribution of strengths for the same fiber coated with silicon. The mean strength for 40 samples was found to be 252 ksi. The distribution for fibers coated with carbon then silicon is shown in figure 3. The mean strength for 41 samples was found to be 282 ksi. Figure 14 shows the strength of fibers coated with silicon then aluminum to be 214 ksi for 34 samples. The strength of fibers coated with carbon then silicon then aluminum is shown in Figure 15. The mean strength for 41 samples was found to be 276 ksi. Figure 16 shows a comparison of the strengths among the coated fibers. From the data it is apparent that there is no significant difference among the fibers tested, all fibers having approximately the same strengths and distributions.

Scanning electron micrographs of the fiber surfaces revealed non-uniform coatings on the fiber surface. The aluminum, on the fibers coated with aluminum, was found to be in islands or blobs on the fiber surface. Figure 17

shows the surface of a fiber coated with silicon then aluminum. The blobs were determined by x-ray analysis to be aluminum. This photograph is representative of all coated fibers. The surface of the uncoated P55 is shown in Figure 18. The flecks on the surface are presumed to be a proprietary sizing that is put on the fiber surface to ensure compatibility with epoxy matrices.

Composites Produced From Coated Fibers

Composites were produced from the coated fibers and a matrix of pure aluminum. Representative heating and cooling curves are shown in figures 8 and 9 respectively. The specimens were designed to 30 volume percent fibers. Figure 19 is representative of all composites produced. Good infiltration pressures were observed for all composites. Table 6 lists the casting conditions for these composites. All composite specimens were cast at temperatures of between 700 and 720 degrees Celsius.

All specimens produced exhibited severe channelling. Apparently as the molten aluminum was forced into the mold containing the fibers, the path of least resistance was taken by the metal. That is, regions where the inter-fiber spacings were relatively large were infiltrated first thus pushing the fibers around in the mold. Figures 20-24 show transverse sections of the composites with the channelling

being quite severe in some specimens.

Figure 25 shows the actual versus rule of mixtures strengths for the composites produced from the coated fibers. The rule of mixtures (ROM) strength is calculated from a fiber strength of 274 ksi and a matrix strength of 10 ksi and is calculated to be 89 ksi. The average strength of composites produced from uncoated fibers was found to be 68 ksi or 76% ROM. The average strength of the composites produced from fibers coated with silicon and aluminum was 53 ksi or 60% ROM. Fibers coated with carbon, silicon, and aluminum yielded composites with an average strength of 48 ksi or 54% ROM. The strength of the composites produced from fibers coated with carbon and silicon was 58 ksi or 65% ROM, while composites produced from fibers coated with silicon led to strengths of 40 ksi or 45% ROM. It is clear that no strengthening occured through the use of any of the coated fibers.

In order to preserve the water soluble reaction products at the interface, the composites produced from coated fibers were polished without the use of water. Absolute ethanol was used as a vehicle for alumina polishing compounds. There appears to be a reaction product at the interface as shown in figure 26. This photograph is of a fiber coated with silicon and is representative of all

composites. The presence of split fibers is observed in this photograph. As the split area is infiltrated with metal, the splitting must have occured early in the fabrication process before solidification perhaps by thermal stresses induced in the fiber during heating or by the pressures of infiltration. All specimens exhibited approximately 5% split fibers.

In order to better see the reaction zone in the composites, an experiment was undertaken to remove the water soluble reaction products and look at where the reaction product had been as an indication of extent of reaction. The composite was placed in a water bath at 80 degrees Celsius for 24 hours. Upon examination, voids around the fiber were indeed observed as seen in figure 27. However, upon further consideration, it was determined that this was not a simple removal of reaction products at the interface but rather a galvanic reaction between the graphite and aluminum. As aluminum is anodic in this system, it is dissolved leaving a void around the fibers. This is in good agreement with the microstructures observed by Cooper et al. [30].

The fracture surfaces of all composites produced were studied. Figure 28, produced from fibers coated with carbon and silicon, shows a fracture surface representative of all composites. Fracture is planar with little pullout

observed. Figure 29 shows a close-up of the fiber in figure xx. The fiber surface appears to be degraded. The structure of the graphite fiber can readily be seen.

Examination of Coated Fibers Leached From Composite

The fibers were leached from the composite using a 1 normal NaOH solution. Lo et al. [31] reports that fibers may be leached from the aluminum matrix by etching in a solution of NaOH or KOH in high purity methanol. This solution proved ineffective in removing the aluminum matrix from the fibers. These leached fibers were gold coated and examined in the scanning electron microscope and are shown in figures 30-34. The fiber surfaces appear to be rough and damaged.

Composites Produced From Various Alloys

In order to further study the effects of interfacial reactions, composites were produced from uncoated Union Carbide P55 graphite fibers and various aluminum alloy matrices. The alloys used were: (1) Al-4.5Cu, (2) Al-2.8Li, (3) Al-7.8Mg, and (4) 357 (7%Si, 0.5 Mg). Table 8 lists casting conditions for the composites produced from these alloys. In order to try to reduce the likelihood of channelling, the fiber volume fraction was increased to approximately 50 percent. It should be noted that attempts to produce composites from the Al-Li alloy were largely

unsuccessful as the reaction of the metal with the mold and crucible was severe. Attempts to infiltrate at the lowest possible temperature resulted in only partially infiltrated composites containing many voids.

Transverse cross sections of the composites produced are shown in figures 35-38. Channelling is still a great problem and is not easily overcome. Table 9 shows the strengths found for the composites produced from the alloy matrices. The strengths of the composites versus ROM strengths are shown graphically in figure 39. The strength of this lot of graphite fibers was tested and found to be 247 ksi and this value was used for the fiber strength in all ROM calculations. The test results are shown in figure 40 The values of the strength of the alloy matrices are taken to be:

Al-2.3Li	30 ksi [32]
Al-4.5Cu	25 ksi [33]
Al-7.8Mg	40 ksi [34]
357	22 ksi [35]

The strength of composites produced from the AL-Li alloy was found to be 51 ksi or 36% ROM. Composites produced from the Al-Cu alloy exhibited a strength of 109 ksi or 81% ROM. The strength of the Al-Si (357) alloy composite was 124 ksi or 93% ROM and the Al-Mg alloy composite strength was 101 ksi or 75% ROM. The transverse strengths obtained

are listed in table 10 and are shown graphically in figure 41. These values are generally low.

Examination of Fibers Leached From Alloy Matrices

Fibers were leached from the composites produced from the alloy matrices and tensile tests performed in order to determine the extent of fiber strength degradation. The strengths of the fibers are summarized in table 15 and shown graphically in figures 42-44. A summary of strengths is shown in figure 45. Fibers from the Al-Li matrix were were not tested due to insufficient lengths of fiber remaining after composite testing. The above is in comparison to the mean strength obtained for the virgin graphite fibers. Figures 46-49 show the surfaces of the leached fibers. Generally, they are rough and appear to be damaged. The fiber strengths exhibited by the leached fibers were not significantly weaker than the virgin fiber, suggesting that damage to the fiber during composite production is minimal for these alloy matrices. Interestingly, when these leached fibers strengths are used for the strength of the fiber in ROM calculations, the ROM strength modified by the leached fiber strength fall within ten percent of observed composite strengths (table 9). This is illustrated in figure 50.

Examination of Composites Produced From Alloy Matrices.

Examination of composites produced from the alloy matrices was undertaken with the intent of observing and measuring the reaction zone thickness. As before, the composites were prepared without being exposed to water. Figures 51-53 show the results of scanning electron microscopy of these specimens. No reaction could be observed in any composite even at magnifications of 37000X. A longitudinal fracture surface is shown in figure 54. This is from the 357 alloy and is representative of all fracture surfaces observed. Additionally, transverse fracture surfaces were also examined and are shown in figures 55-58. All transverse fractures were observed to be interfacial as no fibers were observed to be split. Figure 55 shows Al_4C_3 at the surface of the fiber with crazing of the fiber surface apparent. Reaction products seem to be surrounding all fibers but to a rather limited extent. Conventional metallography was performed on the composite specimens. In the Al-Cu system, theta phase ($CuAl_2$) was found at the fiber surface and confirmed by x-ray analysis. Figures 59 and 60 are micrographs showing this phase at the interface. Similarly, a large amount of second phase can be seen at the fiber surface in the 357 alloy matrix composite. These observations are in agreement with observations of others [36,37]. The second

phase could not be easily detected in the Al-Mg or Al-Li alloys.

CONCLUSIONS

1. Composites were produced from a variety of coated fibers and matrices.

2. Channelling is a problem in all composites produced, however it does not necessarily reduce composite strength.

3. Fibers coated with carbon and silicon were not stronger in the as coated condition than uncoated fibers.

4. Coated fibers recieved were not effective in increasing composite strengths.

5. Production of composites with existing apparatus does not seriously degrade fibers.

6. Production of composites with Al-Li matrix seriously damages the graphite crucible and mold through chemical reaction.

7. Extended contact with water seriously degrades the interface in graphite reinforced aluminum composites by galvanic reaction.

8. Formation of reaction products during processing was minimal and reaction zone could not be detected.

9. Formation of reaction product did not seriously affect composite strengths.

10. As no fibers were observed to be split, failure was interfacial in transverse composites.

11. Failure of longitudinal composites was planar with little pullout observed.

12. Composite strength can be predicted to within 10 percent of actual strength by evaluation of leached fiber strength.

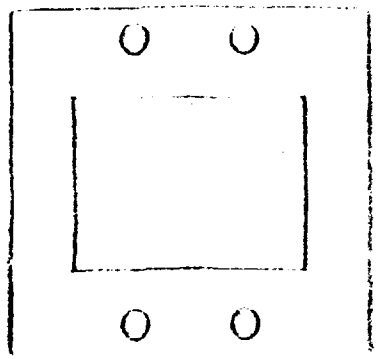

Figure 1. Card used for fiber testing

Figure 2. Fiber testing apparatus

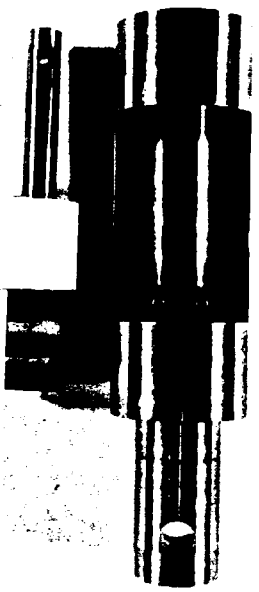

Figure 3. Fiber testing apparatus

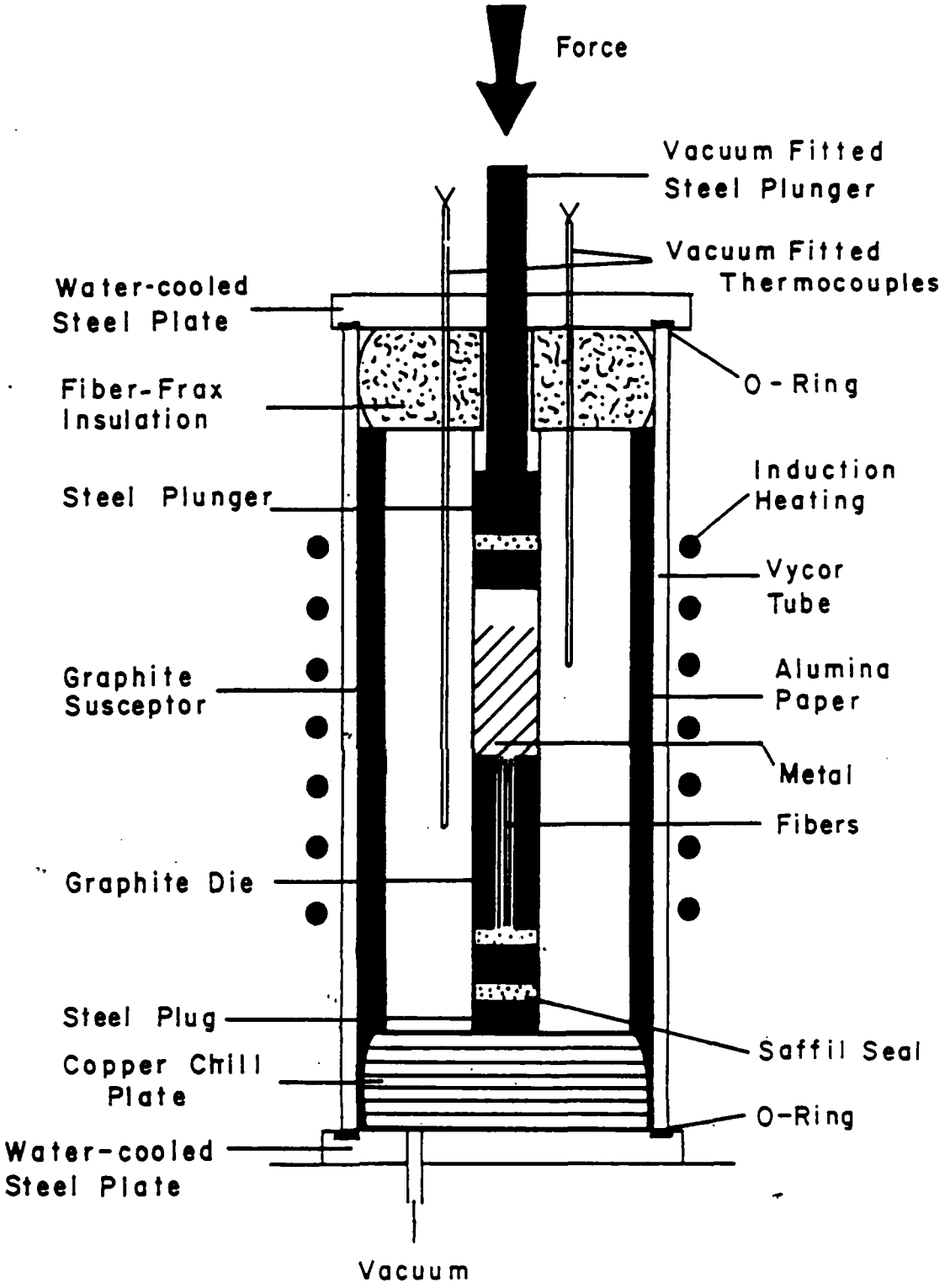

Figure 4. Composite production apparatus

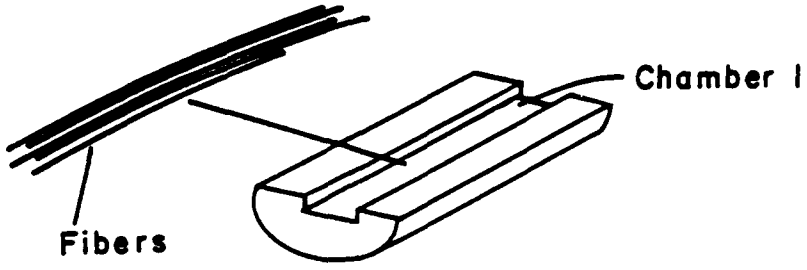

Figure 5. Layup of longitudinal specimen

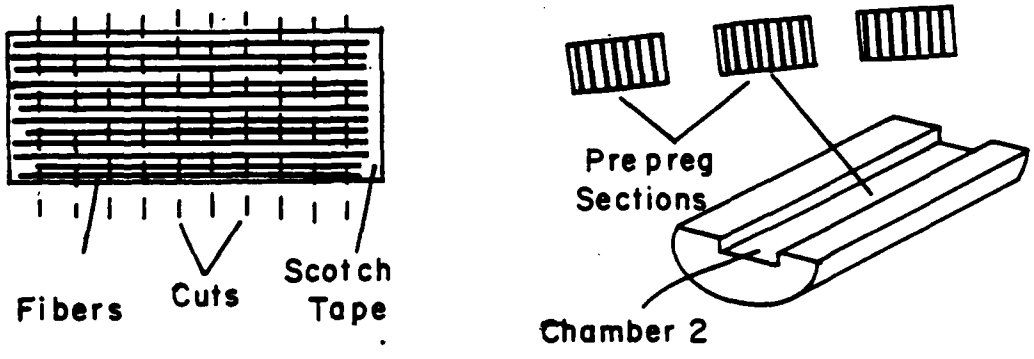

Figure 6. Layup of transverse composite specimen

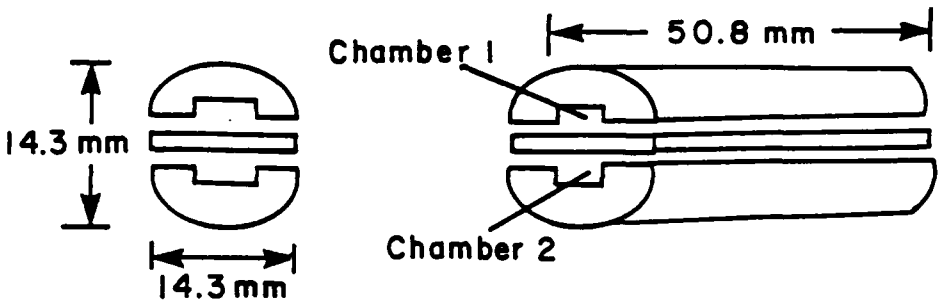

Figure 7. Three piece mold
used for composite production

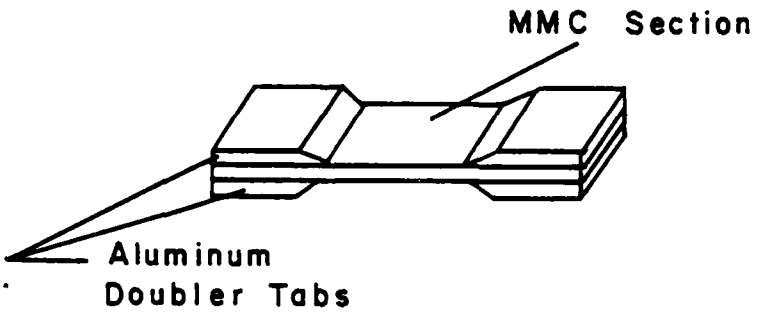

Figure 8. Composite specimen ready for testing

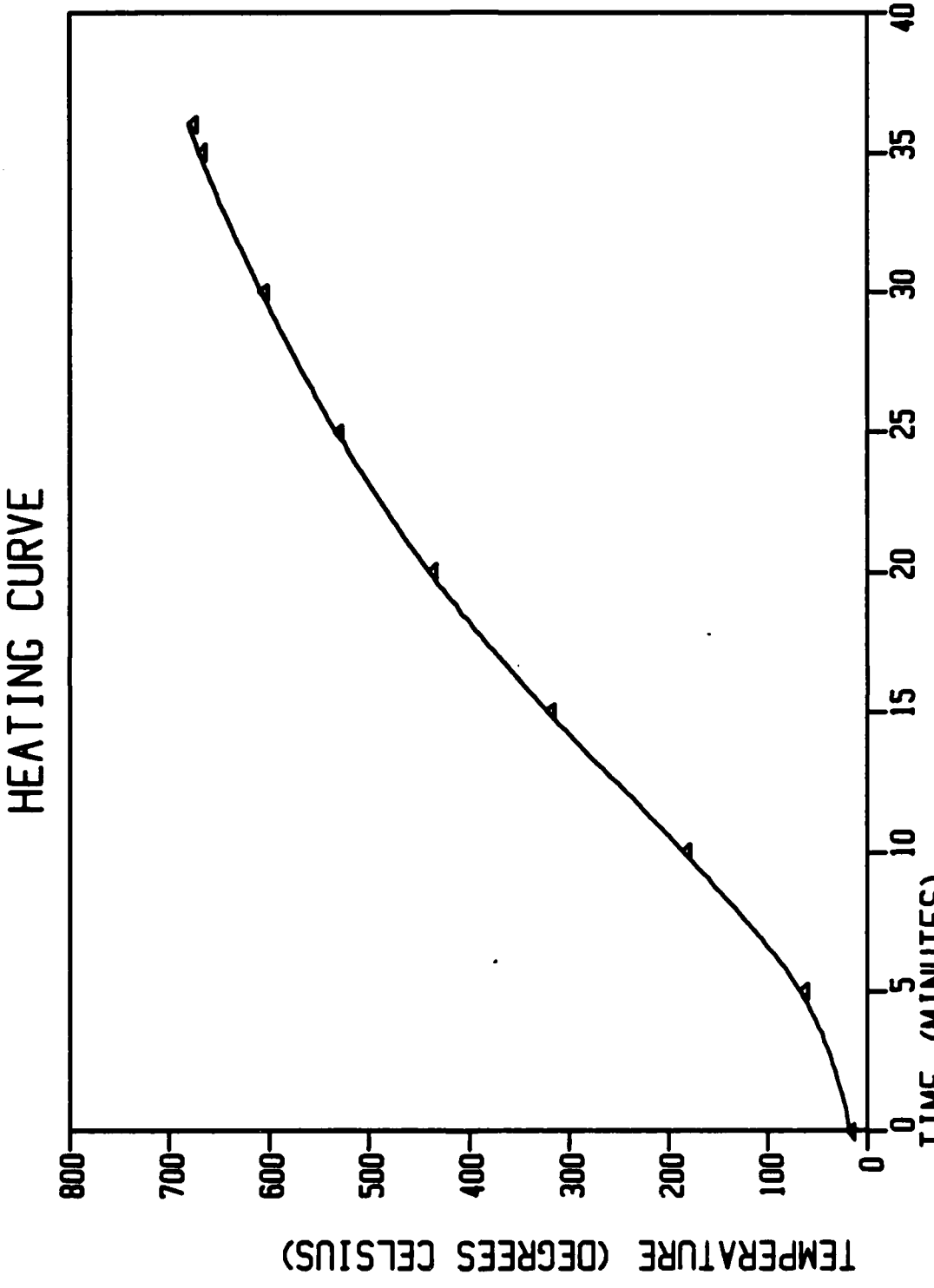

Figure 9. Typical heating curve

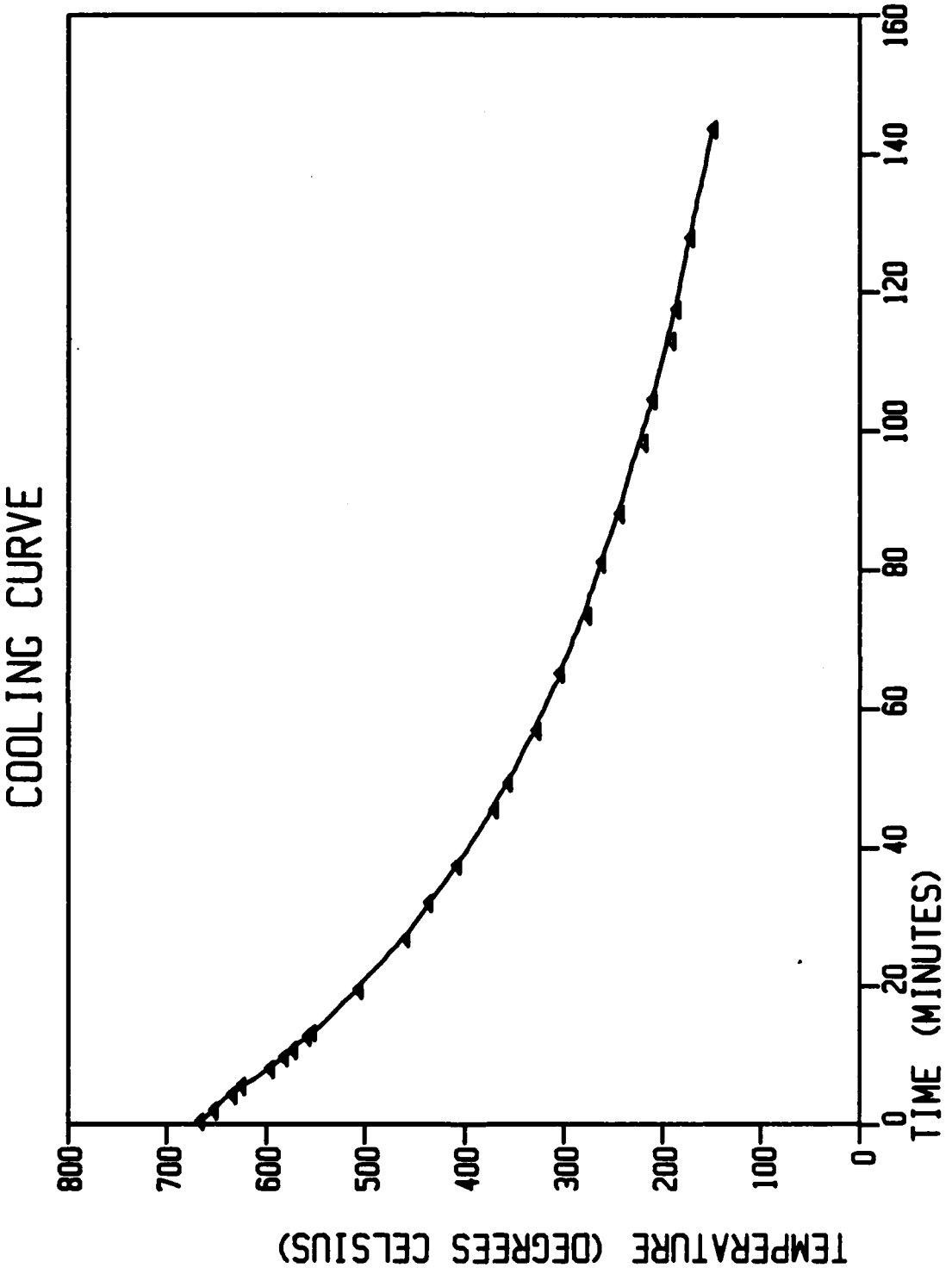

Figure 10. Typical cooling curve

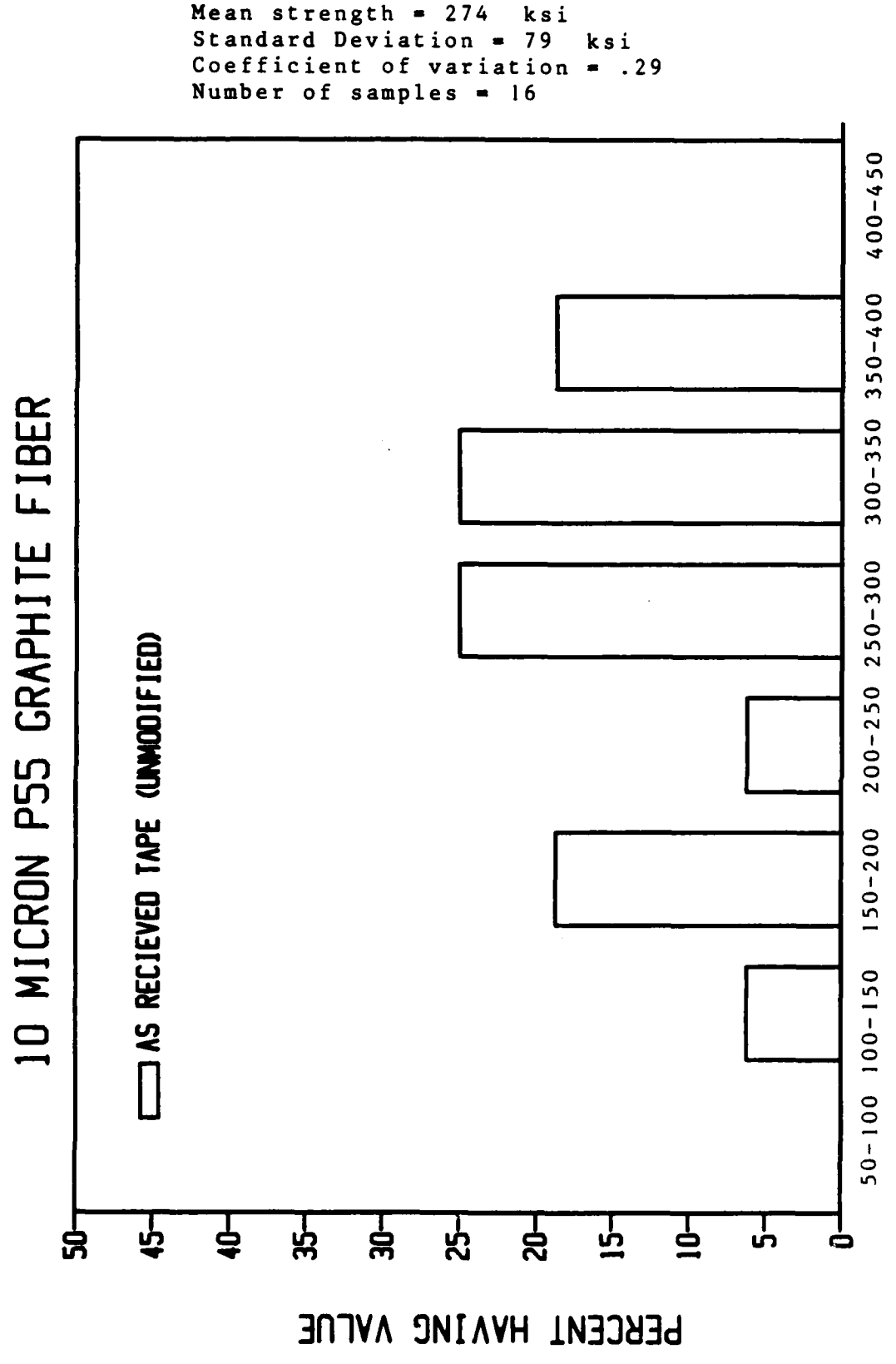
Mean strength = 274 ksi
Standard Deviation = 79 ksi
Coefficient of variation = .29
Number of samples = 16
10 MICRON P55 GRAPHITE FIBER
AS RECIEVED TAPE (UNMODIFIED)
PERCENT HAVING VALUE
0
5
10
15
20
25
30
35
40
45
50
50-100
100-150
150-200
200-250
250-300
300-350
350-400
400-450
ULTIMATE TENSILE STRENGTH (KSI)

Figure 11.

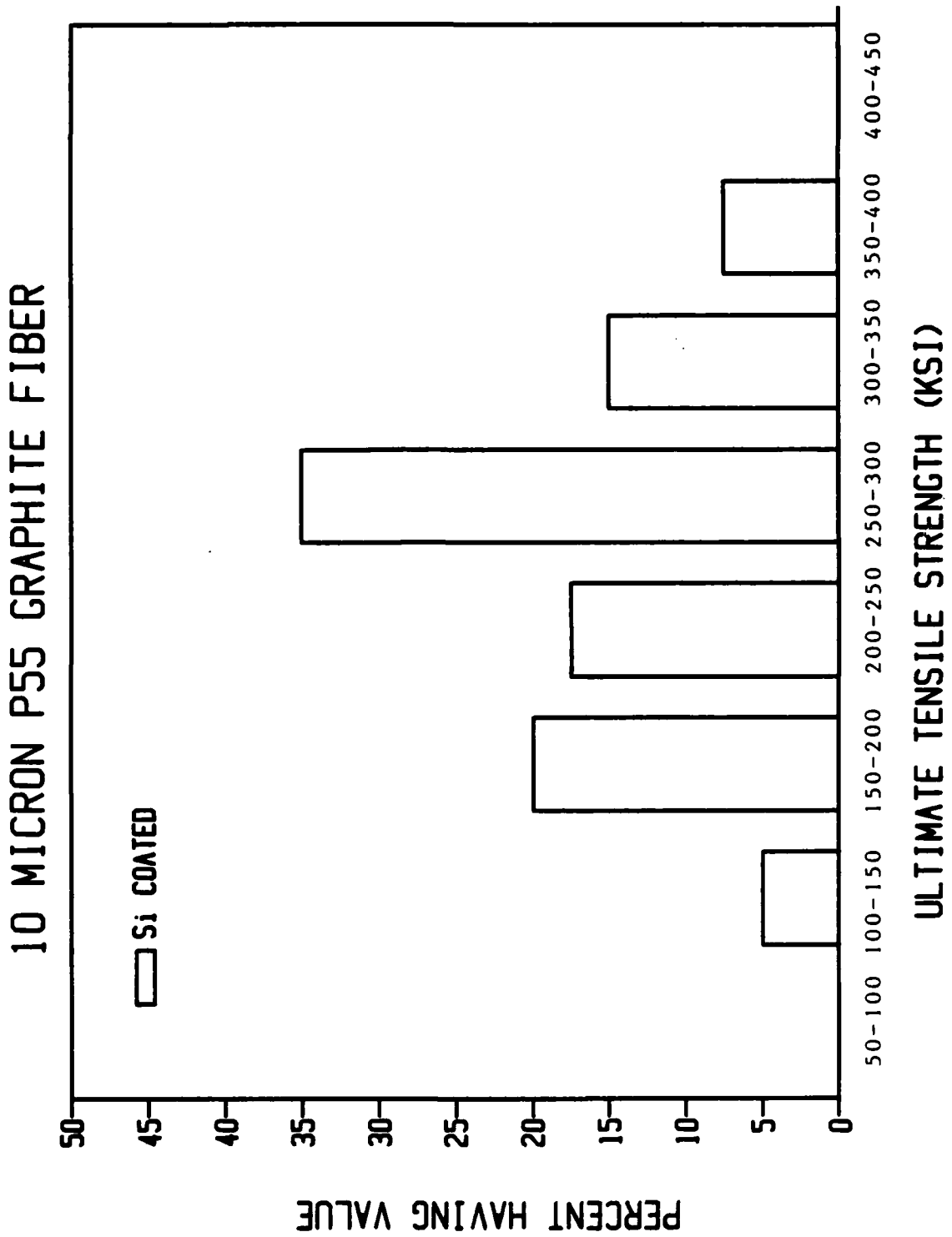
Mean strength = 252 ksi
Standard Deviation = 65 ksi
Coefficient of variation = .26
Number of samples = 40
10 MICRON P55 GRAPHITE FIBER
Si COATED
PERCENT HAVING VALUE
0
5
10
15
20
25
30
35
40
45
50
50-100
100-150
150-200
200-250
250-300
300-350
350-400
400-450
ULTIMATE TENSILE STRENGTH (KSI)

Figure 12.

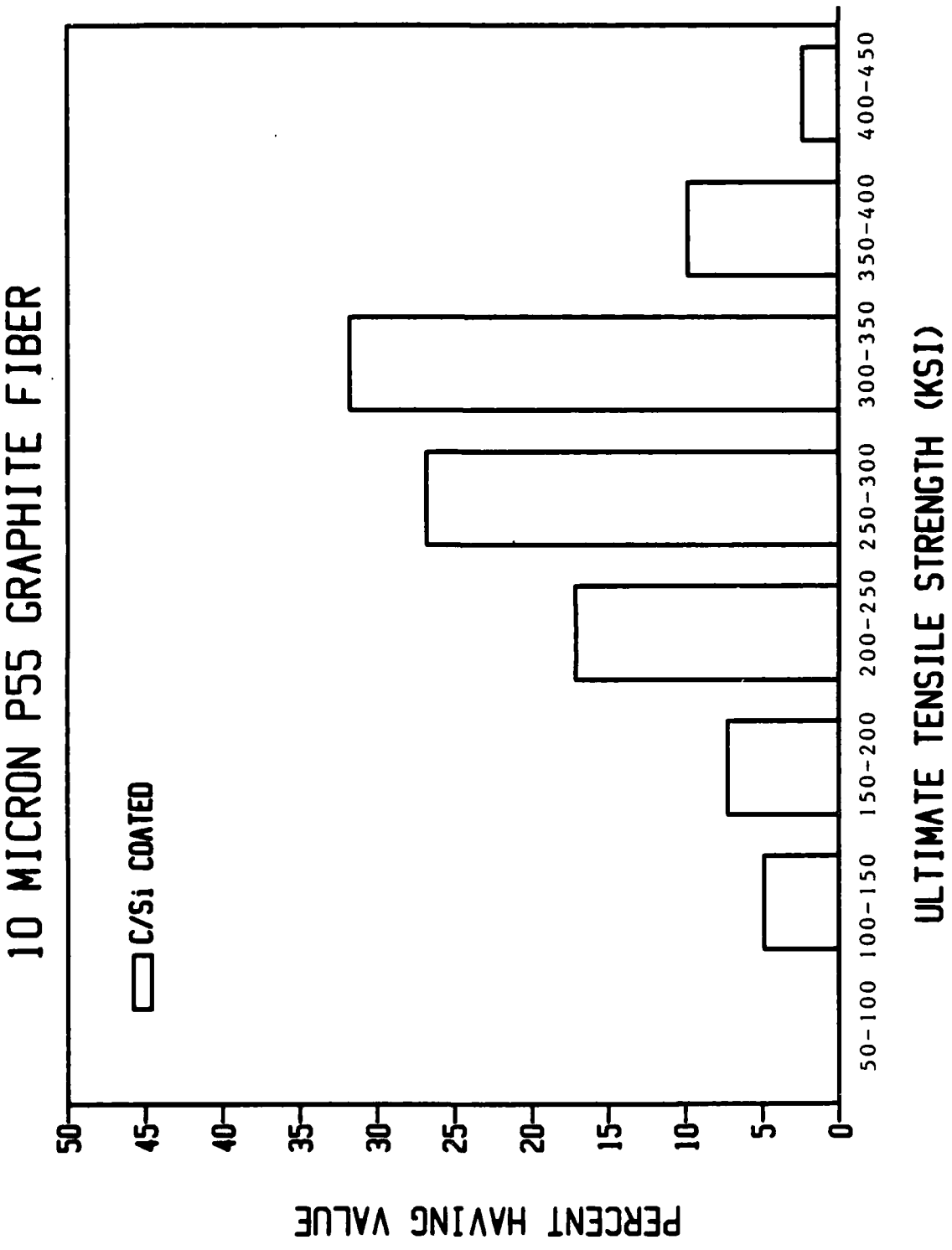
Mean strength = 282 ksi
Standard Deviation = 65 ksi
Coefficient of variation = .23
Number of samples = 41
10 MICRON P55 GRAPHITE FIBER
C/Si COATED
PERCENT HAVING VALUE
0
5
10
15
20
25
30
35
40
45
50
50-100
100-150
150-200
200-250
250-300
300-350
350-400
400-450
ULTIMATE TENSILE STRENGTH (KSI)

Figure 13.

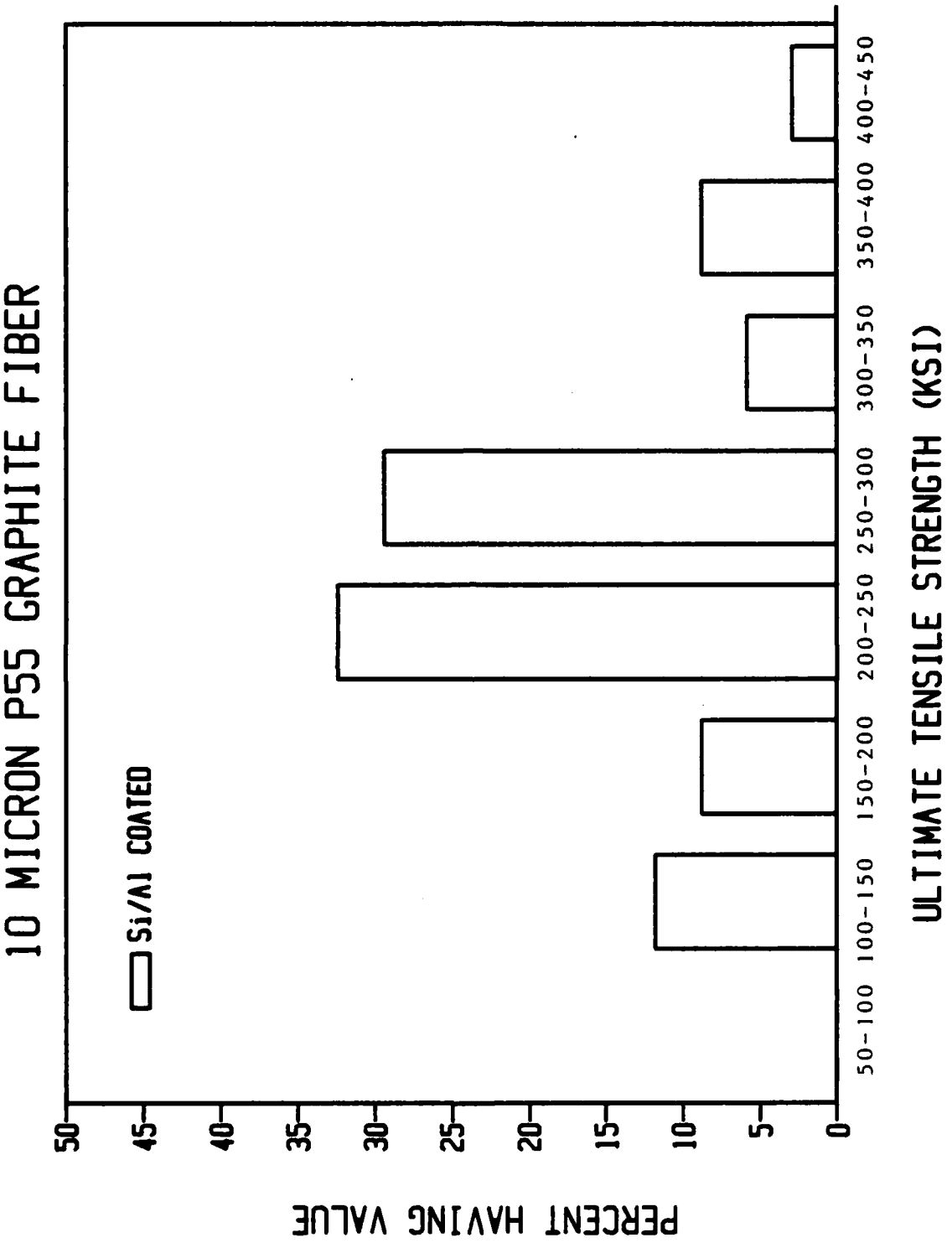
Mean strength = 214 ksi
Standard Deviation = 94 ksi
Coefficient of variation = .44
Number of samples = 34
10 MICRON P55 GRAPHITE FIBER
Si/Al COATED
PERCENT HAVING VALUE
0
5
10
15
20
25
30
35
40
45
50
50-100
100-150
150-200
200-250
250-300
300-350
350-400
400-450
ULTIMATE TENSILE STRENGTH (KSI)

Figure 14.

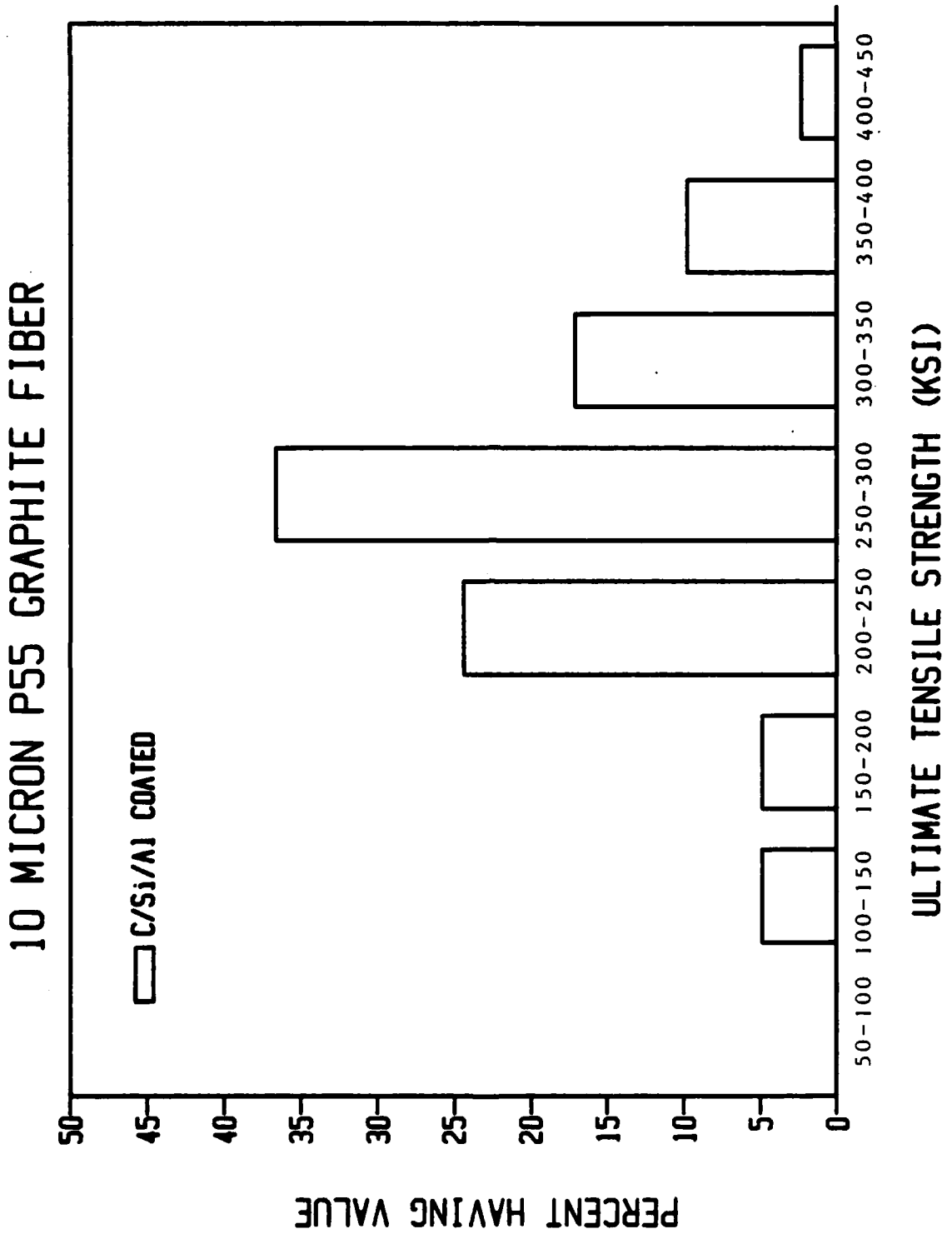
Mean strength = 276 ksi
Standard Deviation = 60 ksi
Coefficient of variation = .22
Number of samples = 41
10 MICRON P55 GRAPHITE FIBER
C/Si/Al COATED
PERCENT HAVING VALUE
0
5
10
15
20
25
30
35
40
45
50
50-100
100-150
150-200
200-250
250-300
300-350
350-400
400-450
ULTIMATE TENSILE STRENGTH (KSI)

Figure 15.

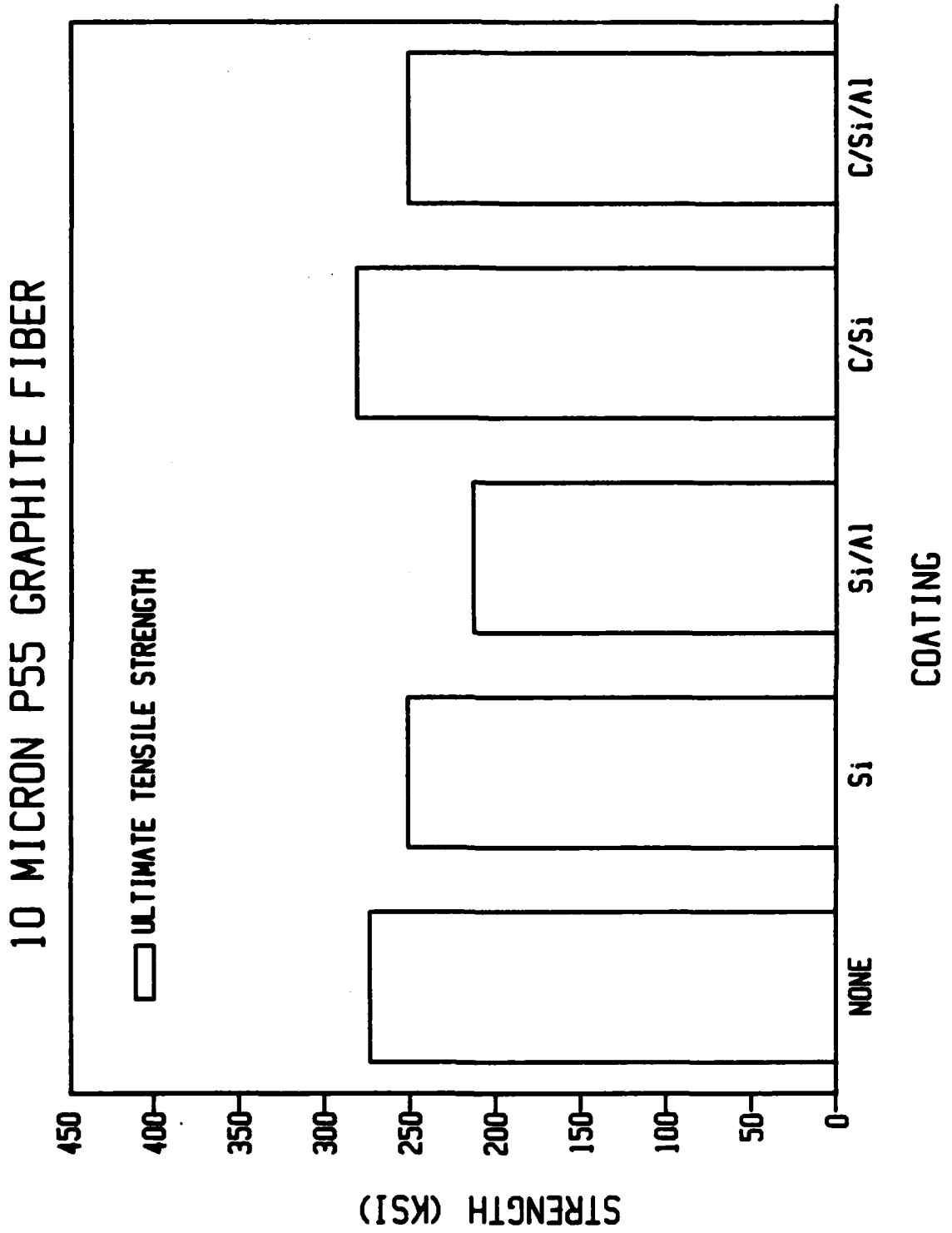

Figure 16. Comparison of coated fiber strengths

Figure 17. Surface of fiber coated with silicon and aluminum (4900x)

Figure 18. Uncoated P55 fiber (840x)

Figure 19. Typical composite specimen

Figure 20. Transverse section of composite produced from uncoated fiber

Figure 21. Transverse section of composite produced from silicon coated fiber

Figure 22. Transverse section of composite produced from carbon-silicon coated fiber

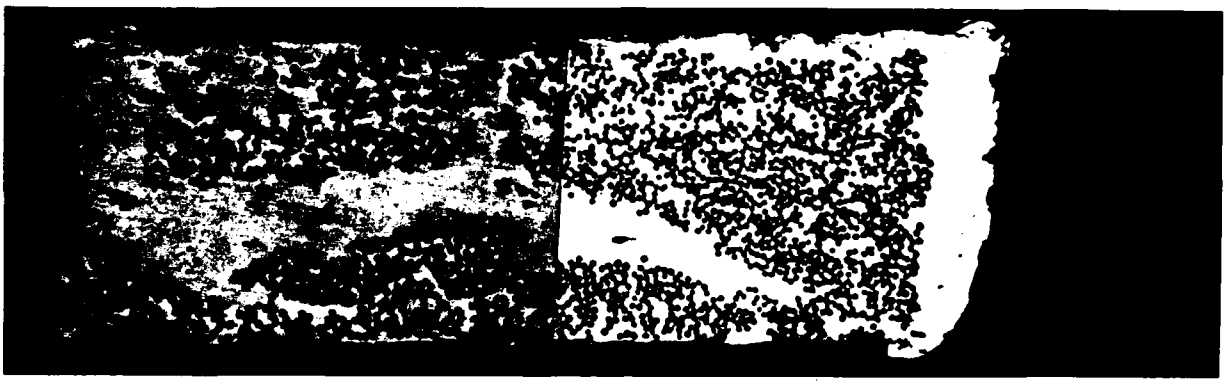

Figure 23. Transverse section of composite produced from silicon-aluminum coated fiber

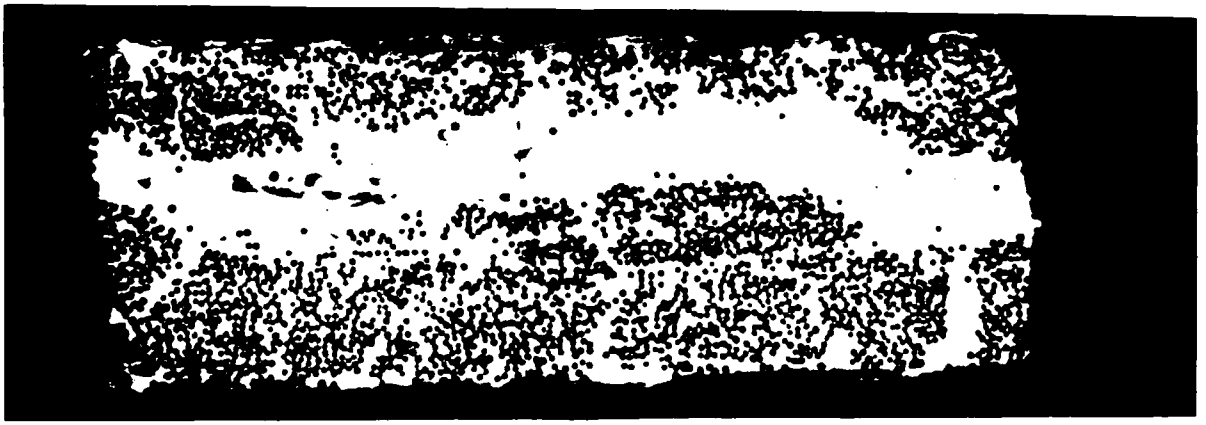

Figure 24. Transverse section of composite produced from carbon-silicon-aluminum coated fiber

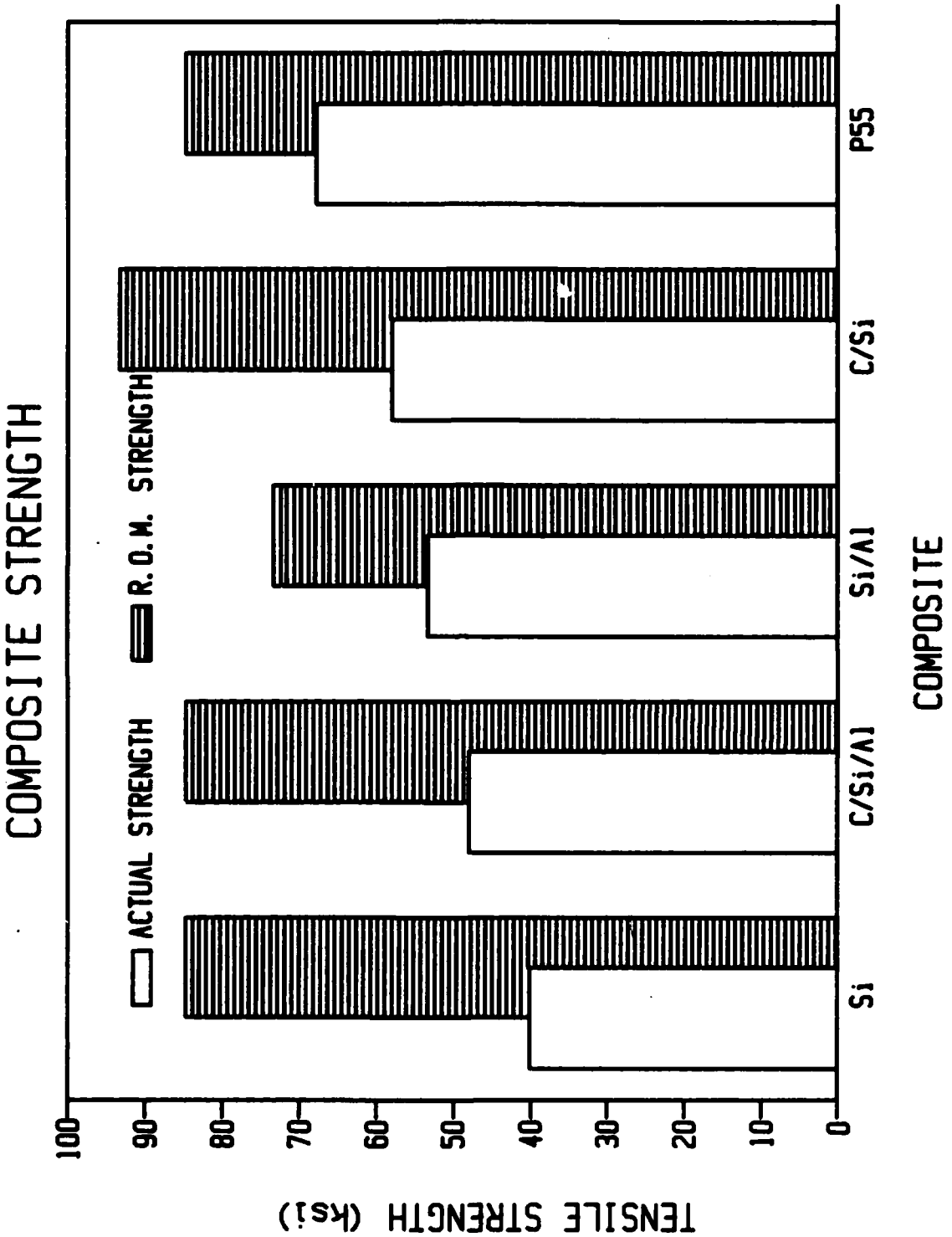

Figure 25. Actual vs. ROM strength for composites produced from coated fibers

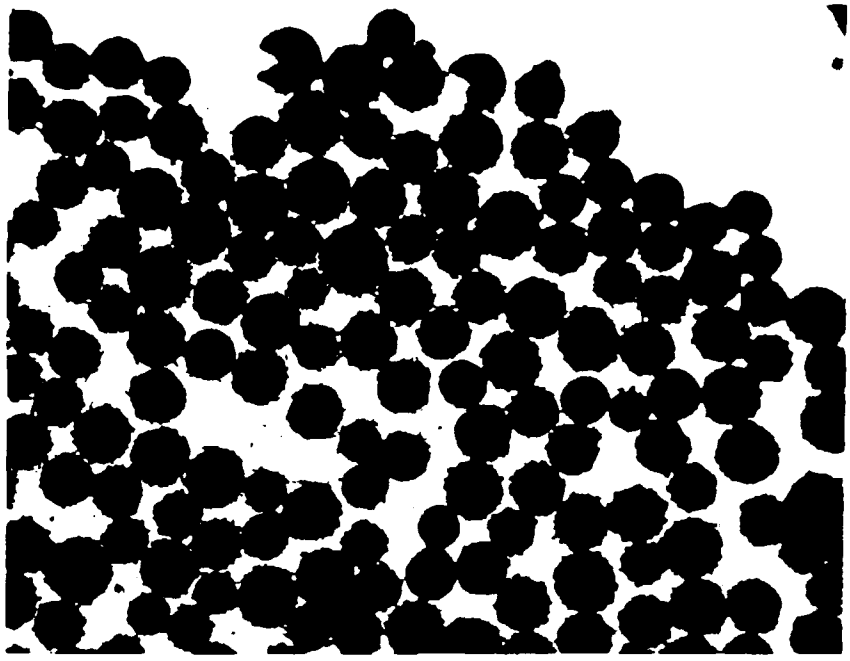

Figure 26. Composite microstructure showing reaction product at interface (600x)

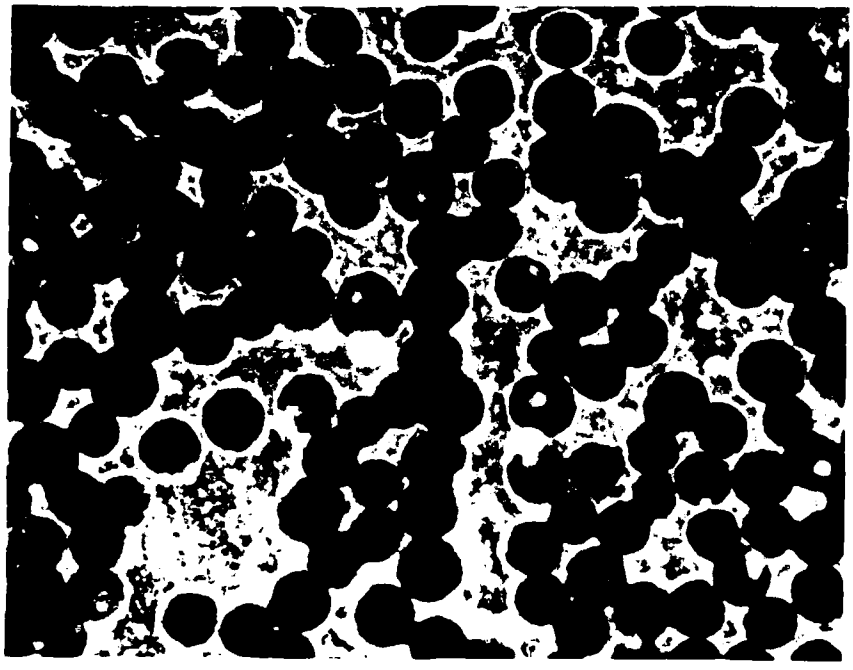

Figure 27. Composite microstructure showing voids around fibers (600x)

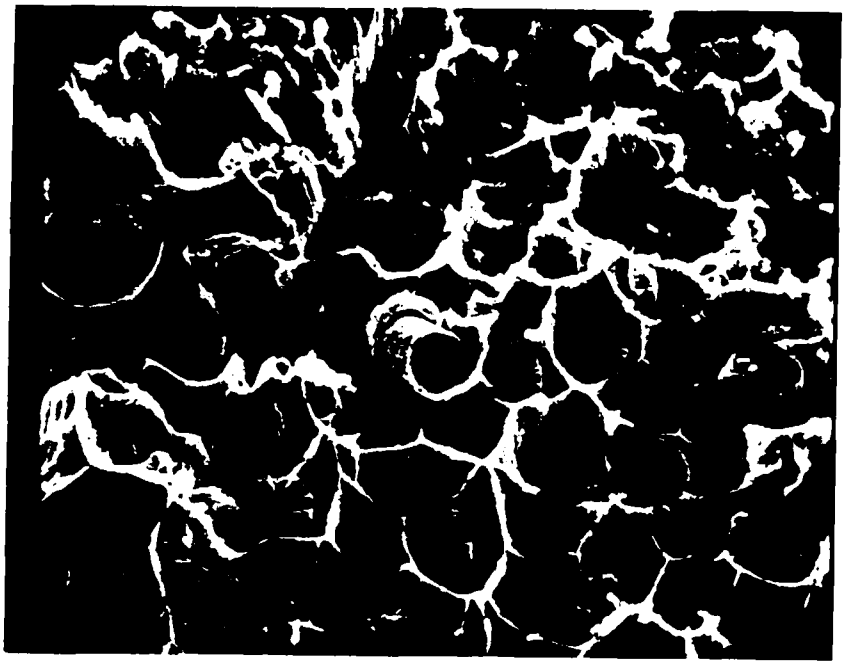

Figure 28. Typical fracture surface (950x)

Figure 29. Pulled-out fiber in composite (4750x)

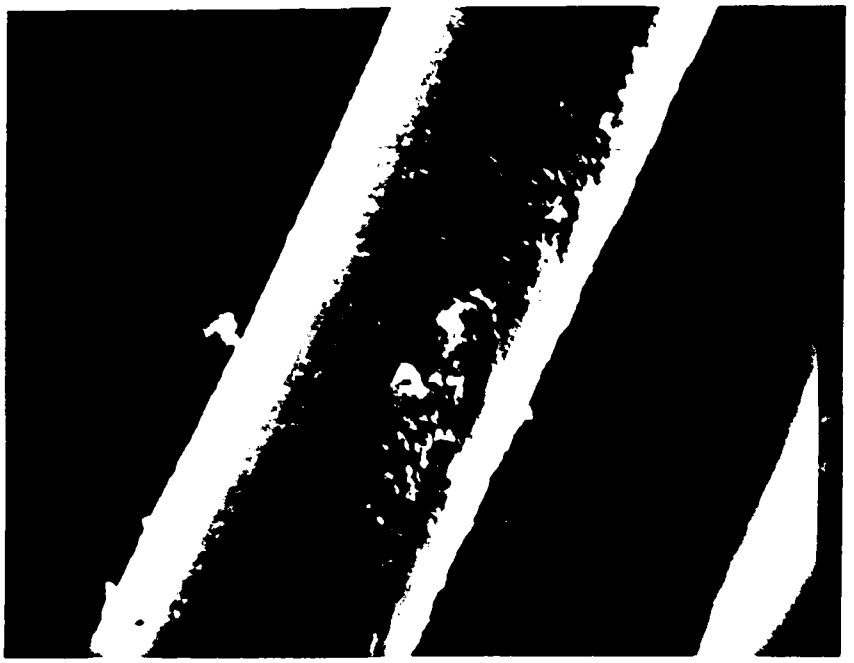

Figure 30. Uncoated fiber leached from composite

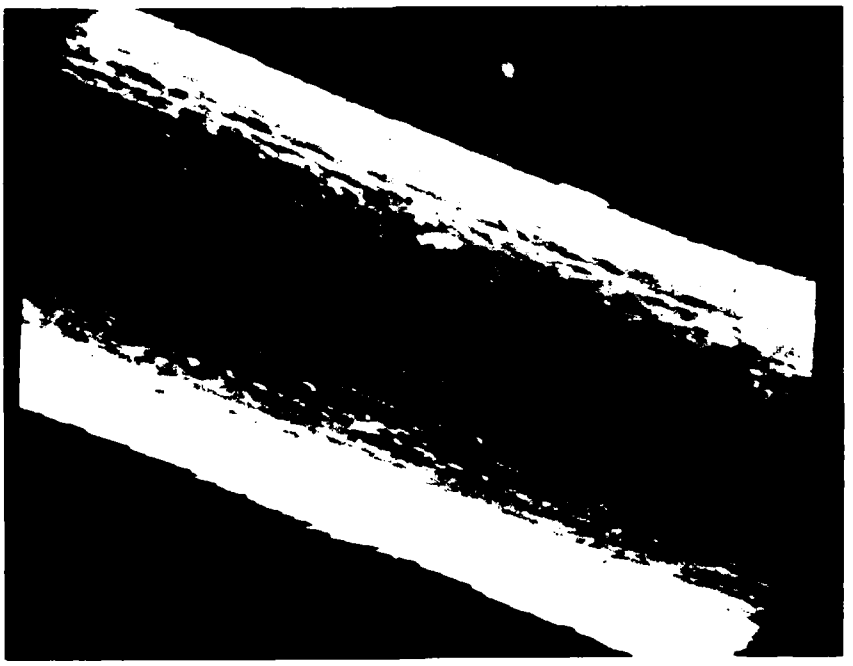

Figure 31. Silicon coated fiber leached from composite

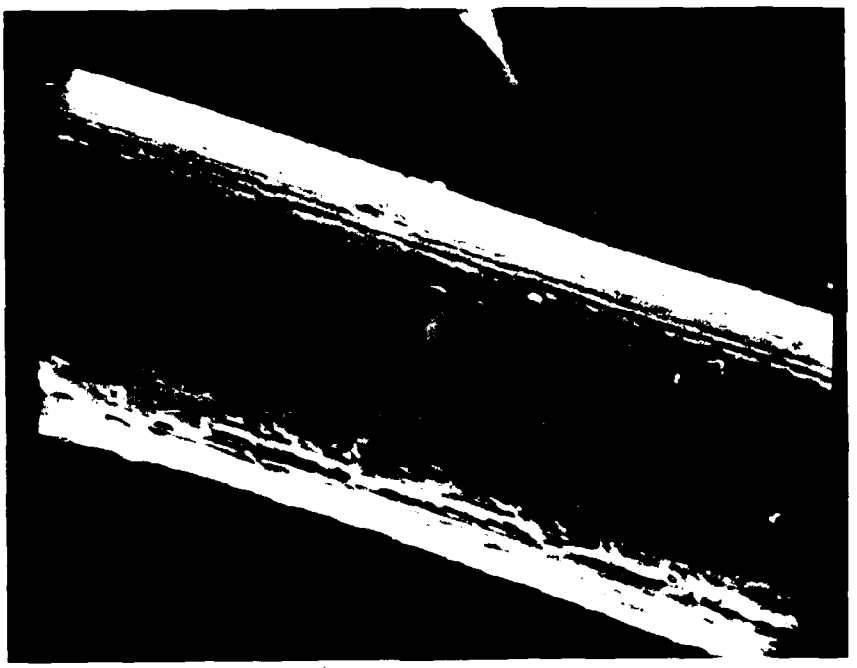

Figure 32. Carbon-silicon coated fiber leached from composite

Figure 33. Silicon-aluminum coated fiber leached from composite

Figure 34. Carbon-silicon-aluminum coated fiber leached from composite

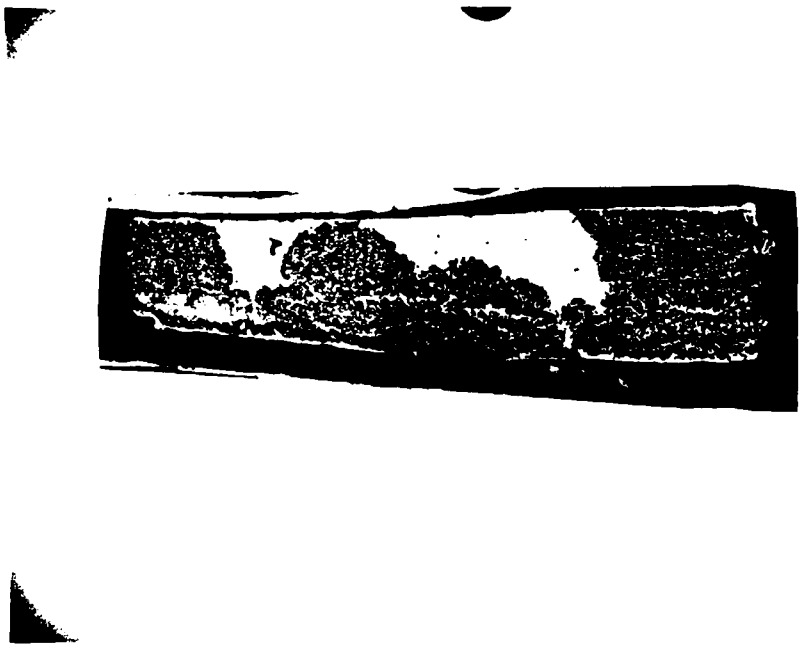

Figure 35. Transverse section of composite with Al-Si alloy matrix

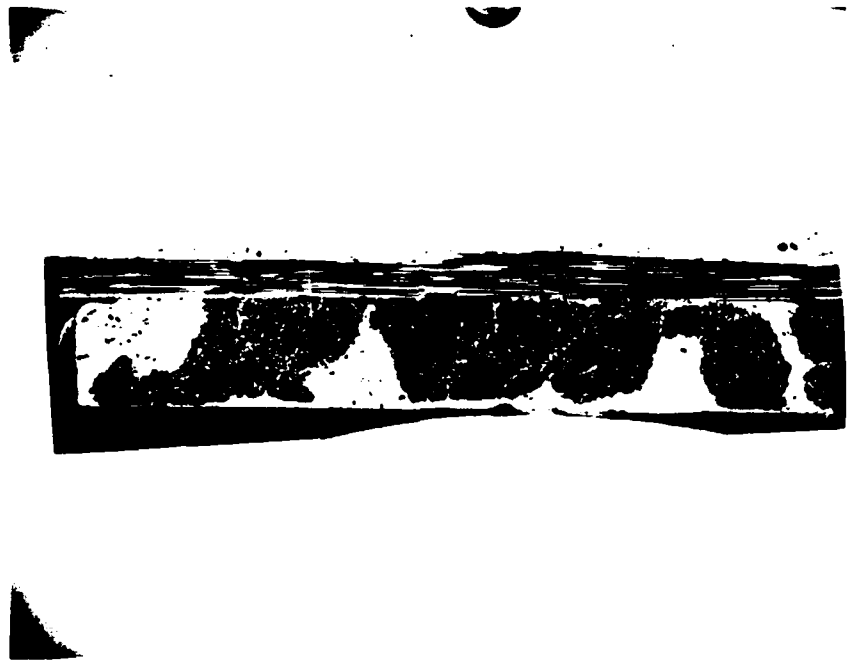

Figure 36. Transverse section of composite with Al-Li alloy matrix

Figure 37. Transverse section of composite with Al-Cu alloy matrix

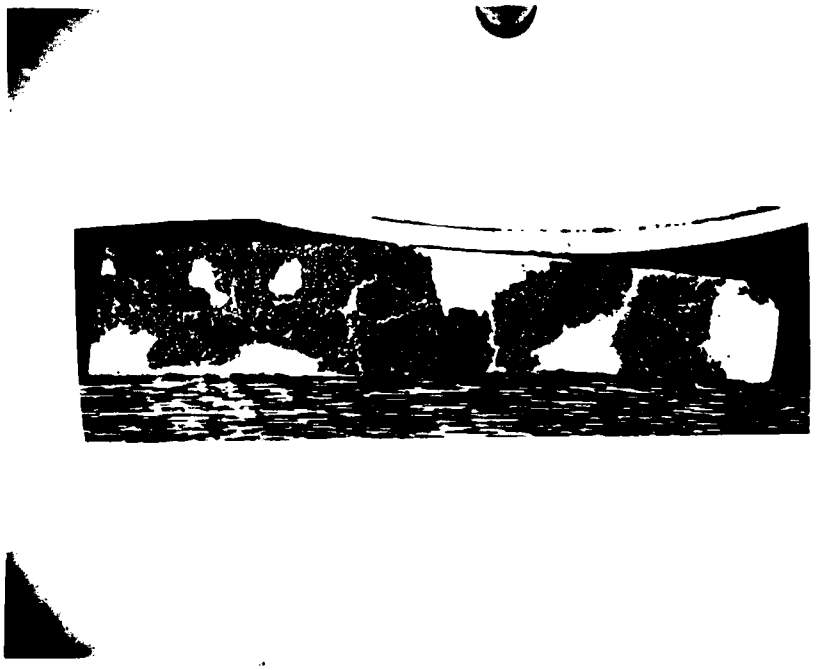

Figure 38. Transverse section of composite with Al-Mg alloy matrix

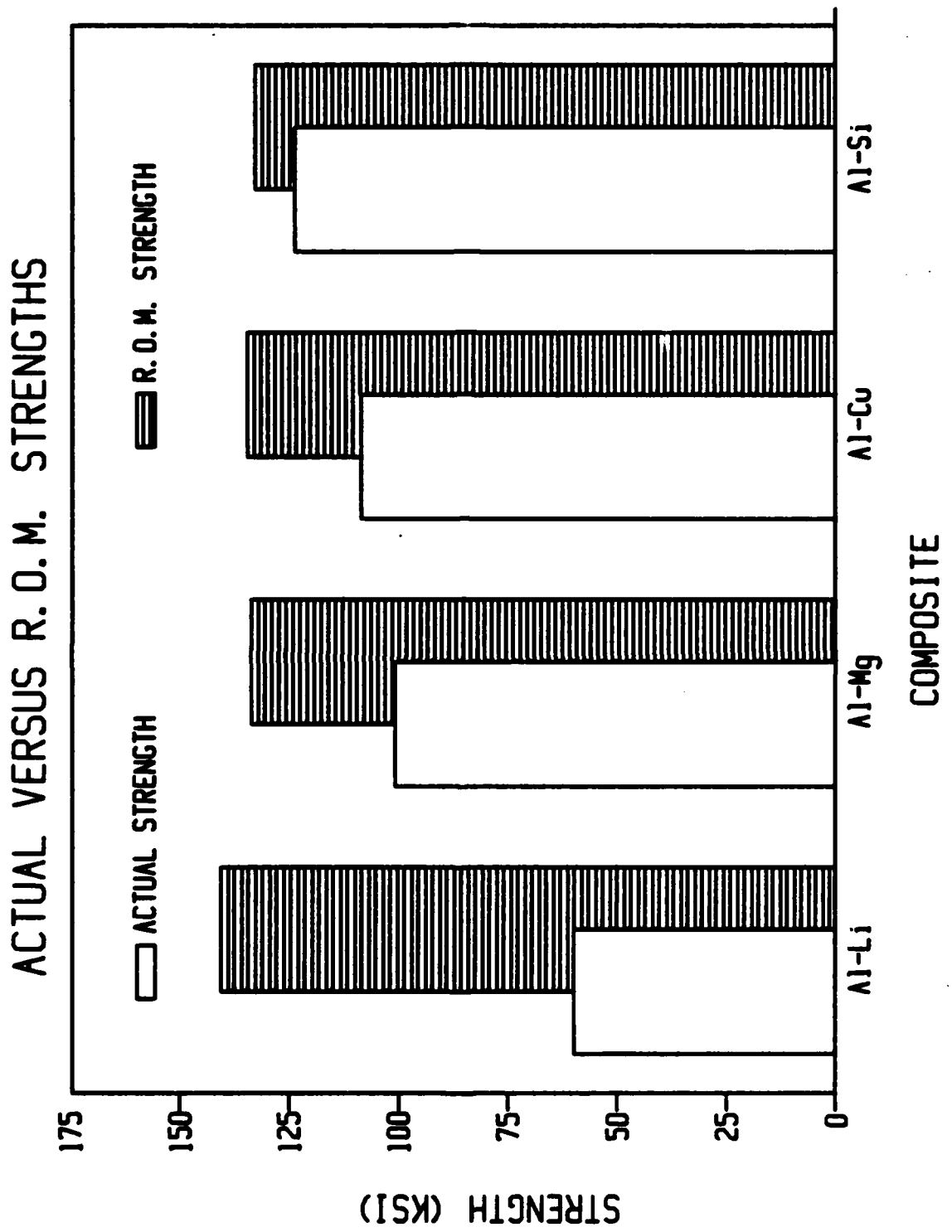

Figure 39. Actual vs. ROM strengths for alloy matrix composites

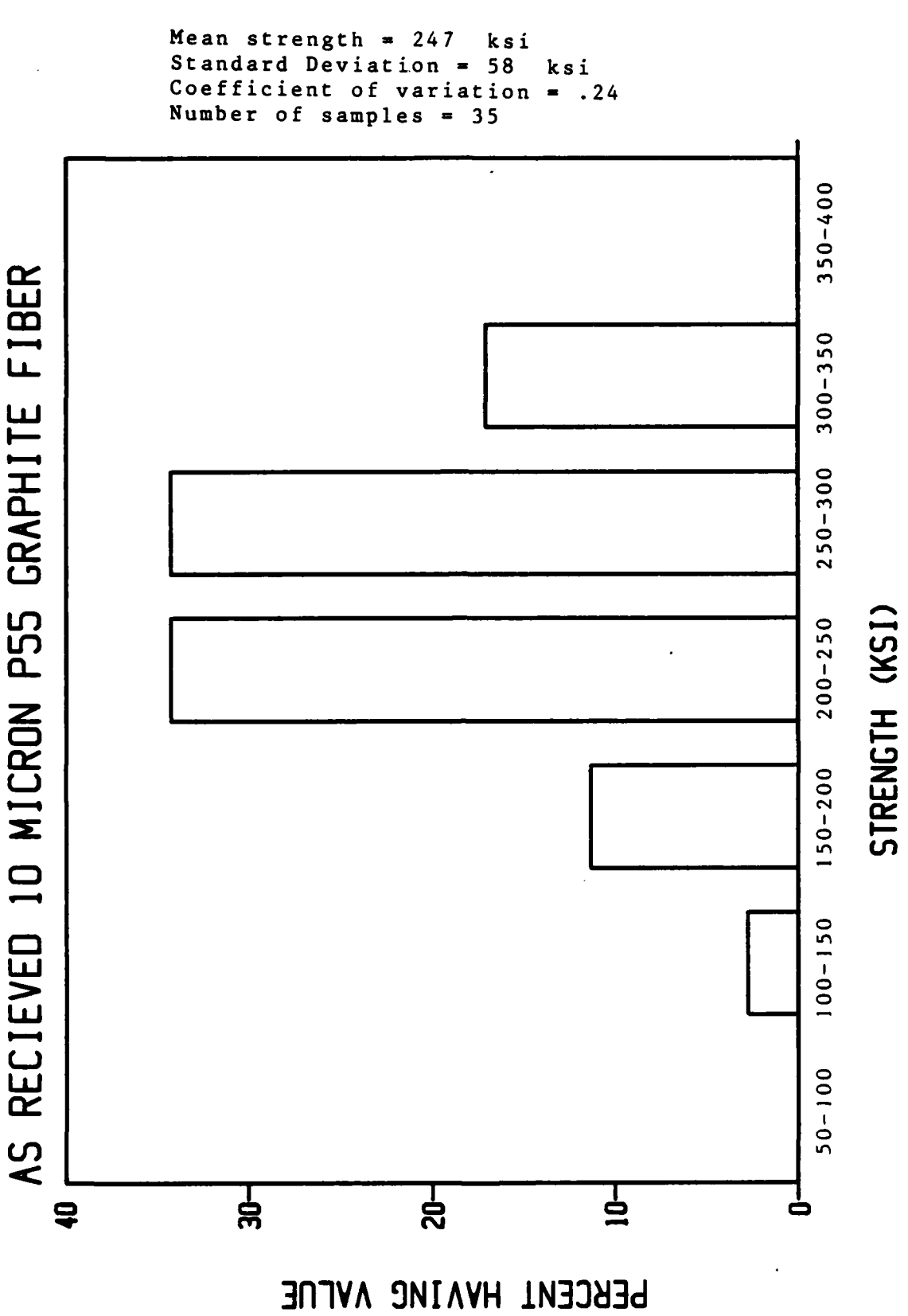
Mean strength = 247 ksi
Standard Deviation = 58 ksi
Coefficient of variation = .24
Number of samples = 35
AS RECIEVED 10 MICRON P55 GRAPHITE FIBER
PERCENT HAVING VALUE
0
10
20
30
40
50-100
100-150
150-200
200-250
250-300
300-350
350-400
STRENGTH (KSI)

Figure 40.

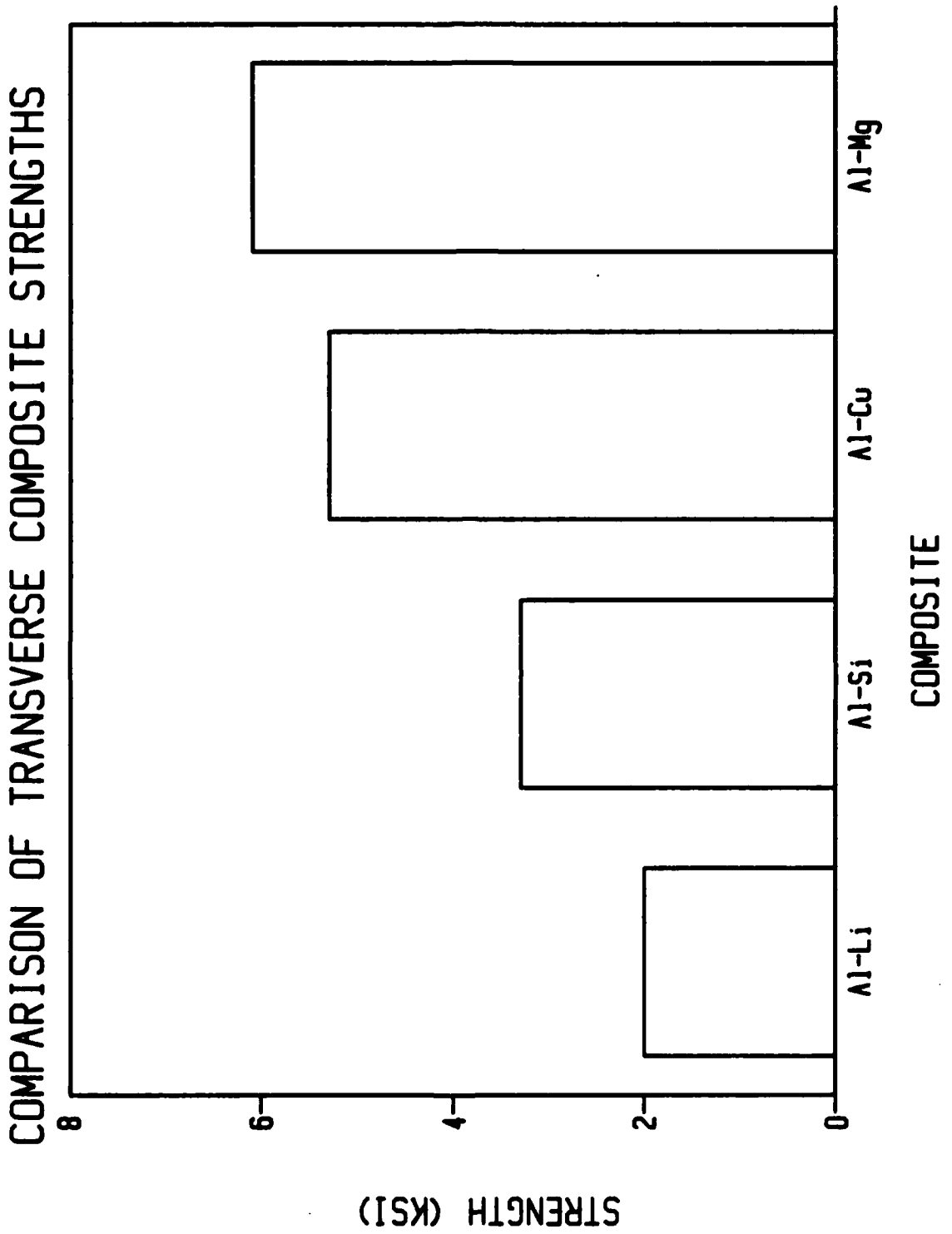
COMPARISON OF TRANSVERSE COMPOSITE STRENGTHS
STRENGTH (KSI)
0
2
4
6
8
Al-Li
Al-Si
Al-Cu
Al-Mg
COMPOSITE

Figure 41.

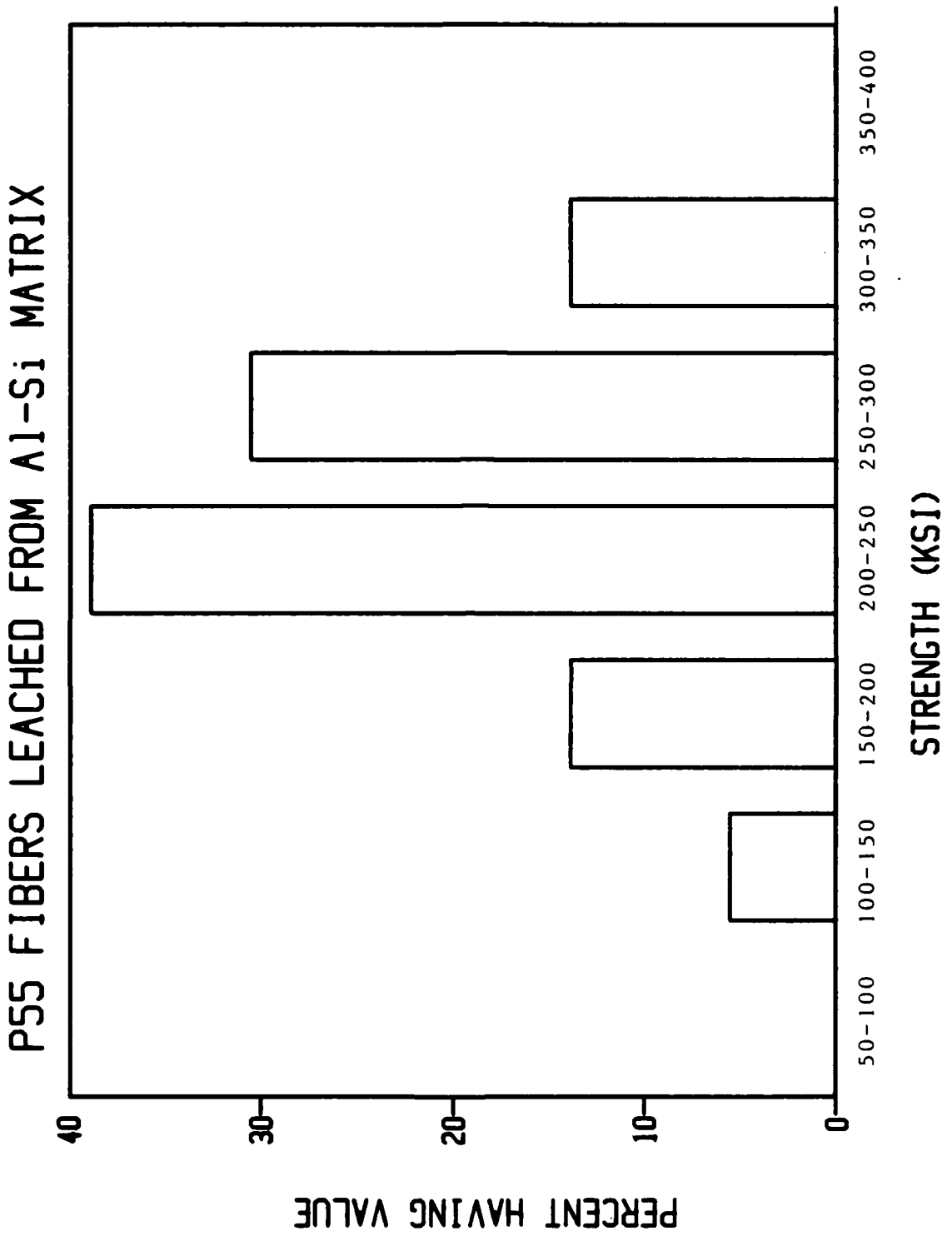
Mean strength = 243 ksi
Standard Deviation = 49 ksi
Coefficient of variation = .2
Number of samples = 36
P55 FIBERS LEACHED FROM Al-Si MATRIX
PERCENT HAVING VALUE
0
10
20
30
40
50-100
100-150
150-200
200-250
250-300
300-350
350-400
STRENGTH (KSI)

Figure 42.

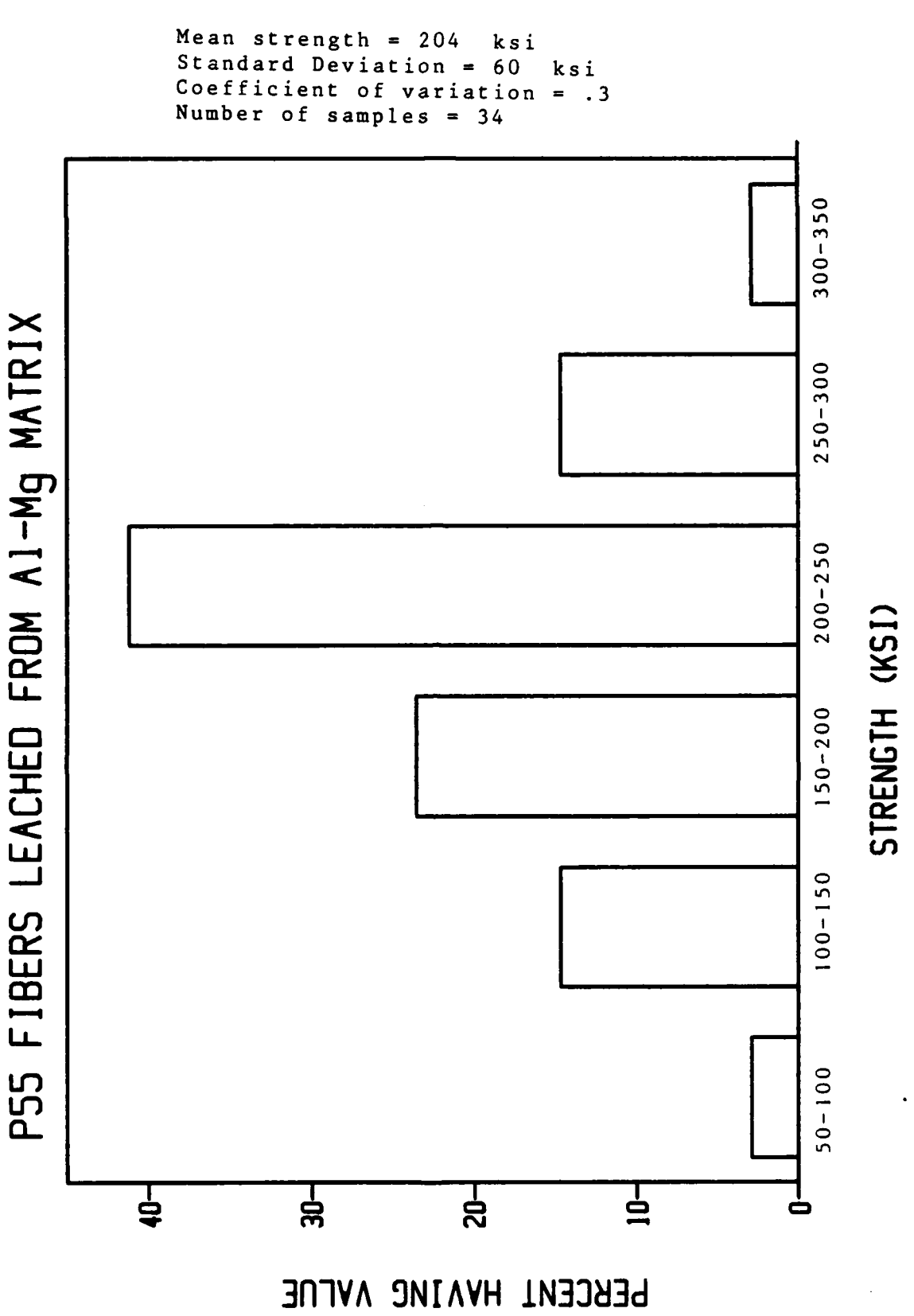
Mean strength = 204 ksi
Standard Deviation = 60 ksi
Coefficient of variation = .3
Number of samples = 34
P55 FIBERS LEACHED FROM Al-Mg MATRIX
PERCENT HAVING VALUE
0
10
20
30
40
50-100
100-150
150-200
200-250
250-300
300-350
STRENGTH (KSI)

Figure 43.

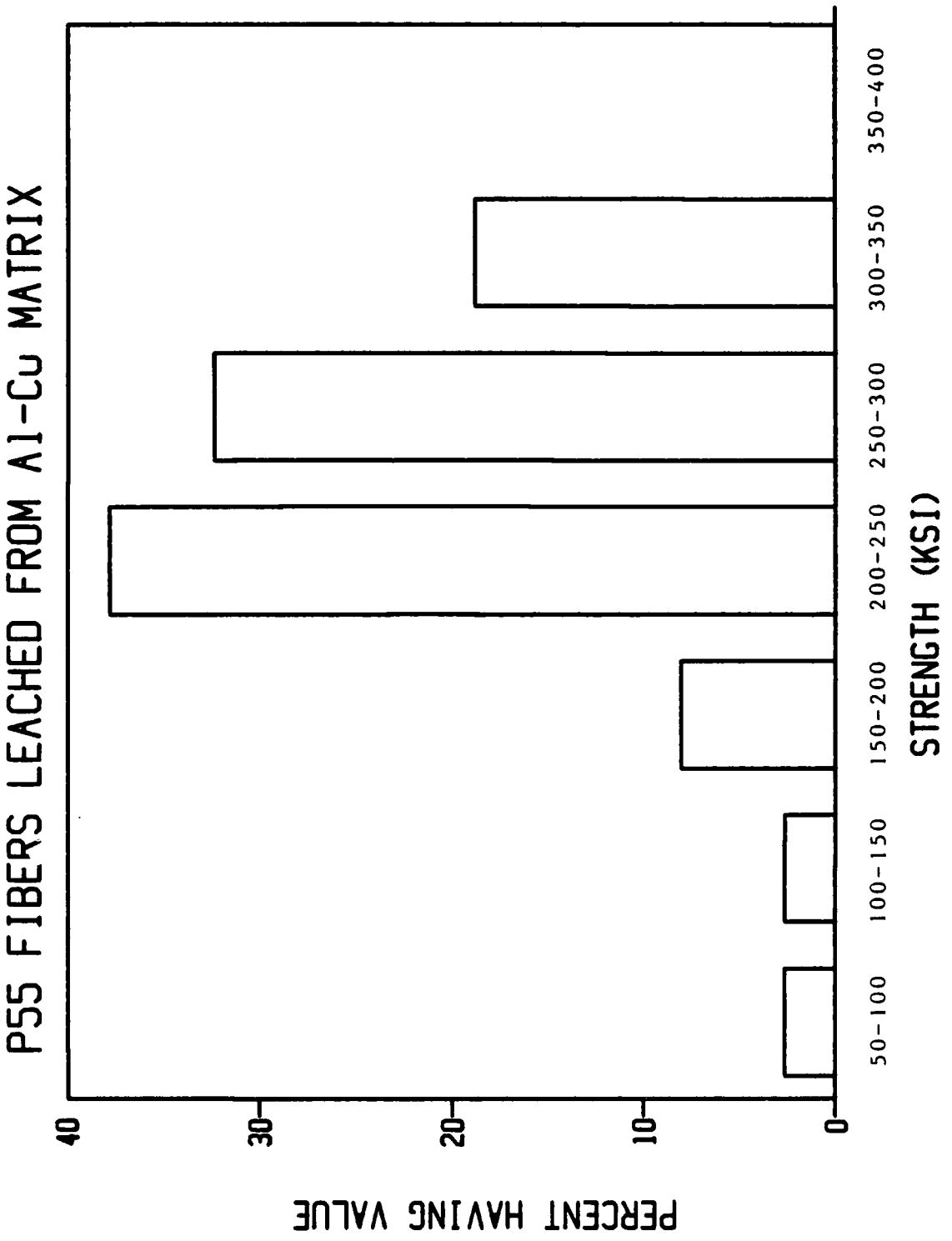
Mean strength = 217 ksi
Standard Deviation = 69 ksi
Coefficient of variation = .32
Number of samples = 37
P55 FIBERS LEACHED FROM Al-Cu MATRIX
PERCENT HAVING VALUE
0
10
20
30
40
50-100
100-150
150-200
200-250
250-300
300-350
350-400
STRENGTH (KSI)

Figure 44.

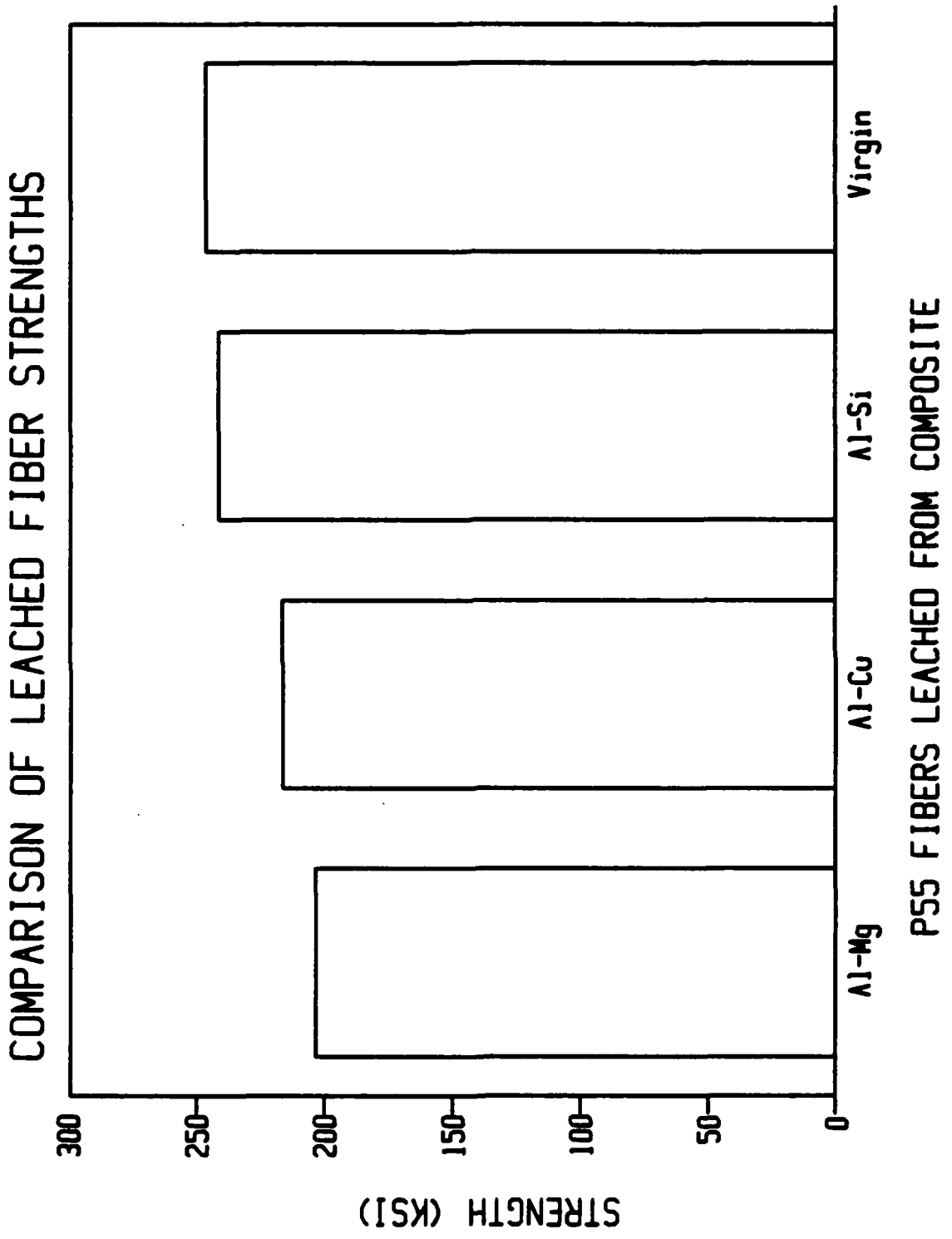

Figure 45. Summary of fiber strengths leached from alloy matrices

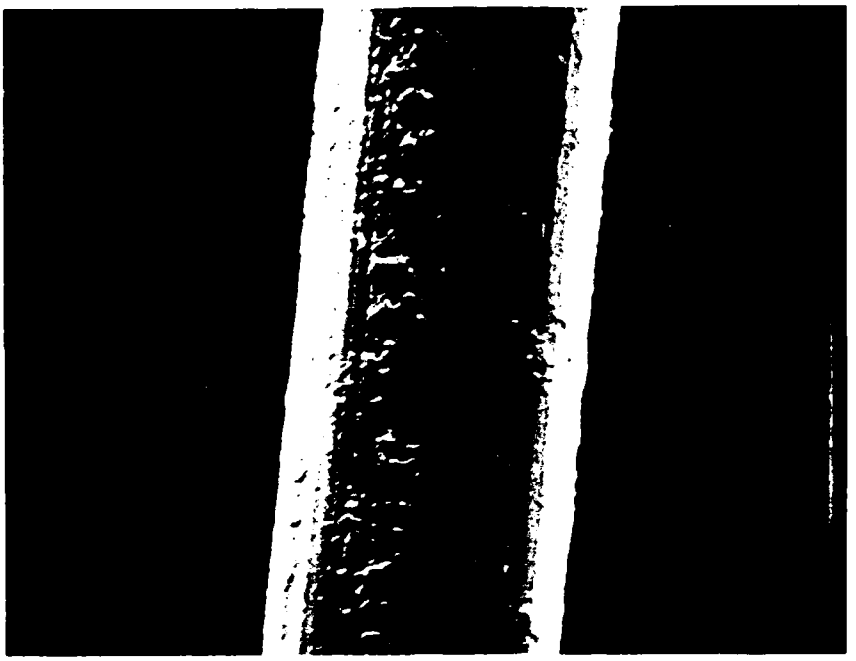

Figure 46. Typical surface of fiber leached from Al-Li alloy

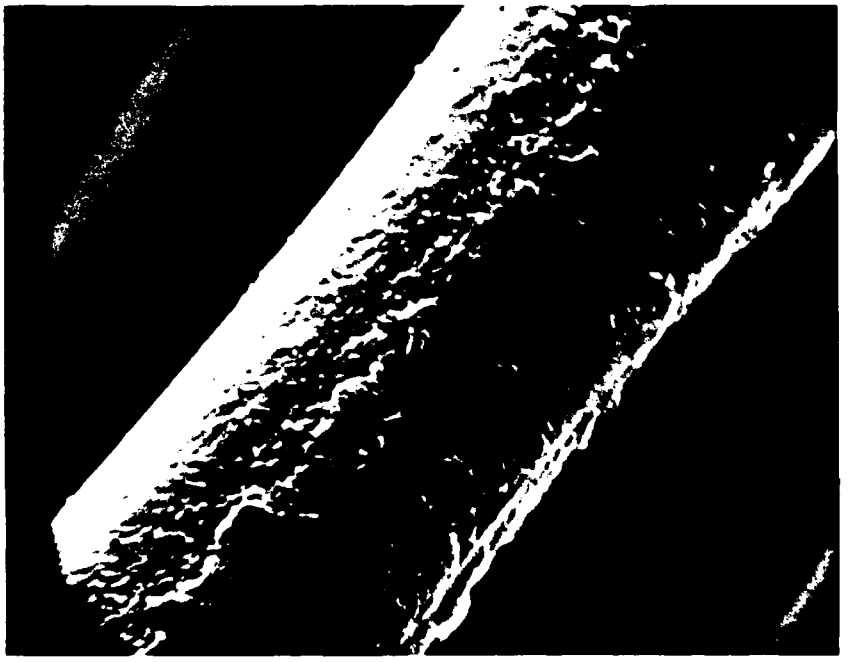

Figure 47. Typical surface of fiber leached from Al-Cu alloy

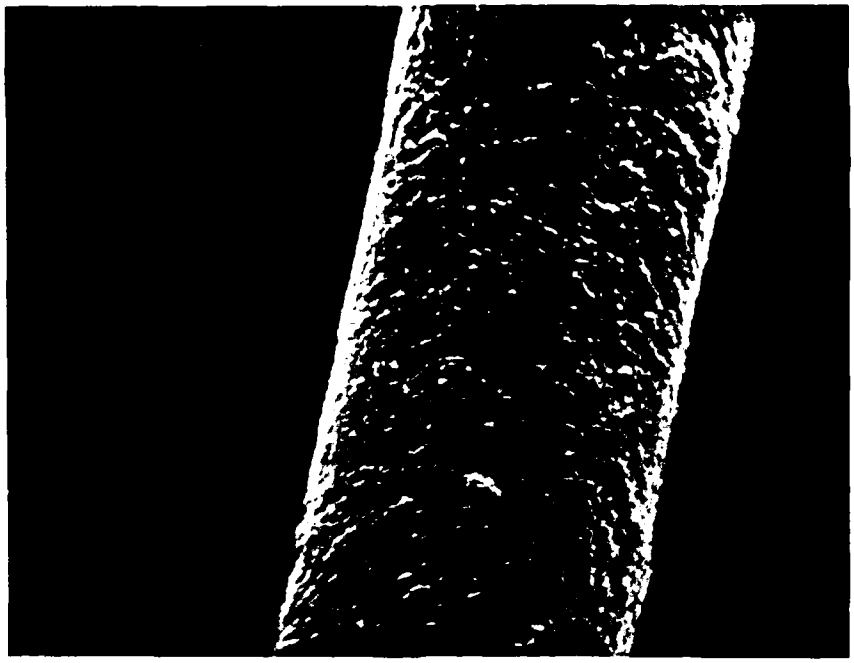

Figure 48. Typical surface of fiber leached from Al-Mg alloy

Figure 49. Typical surface of fiber leached from Al-Si alloy

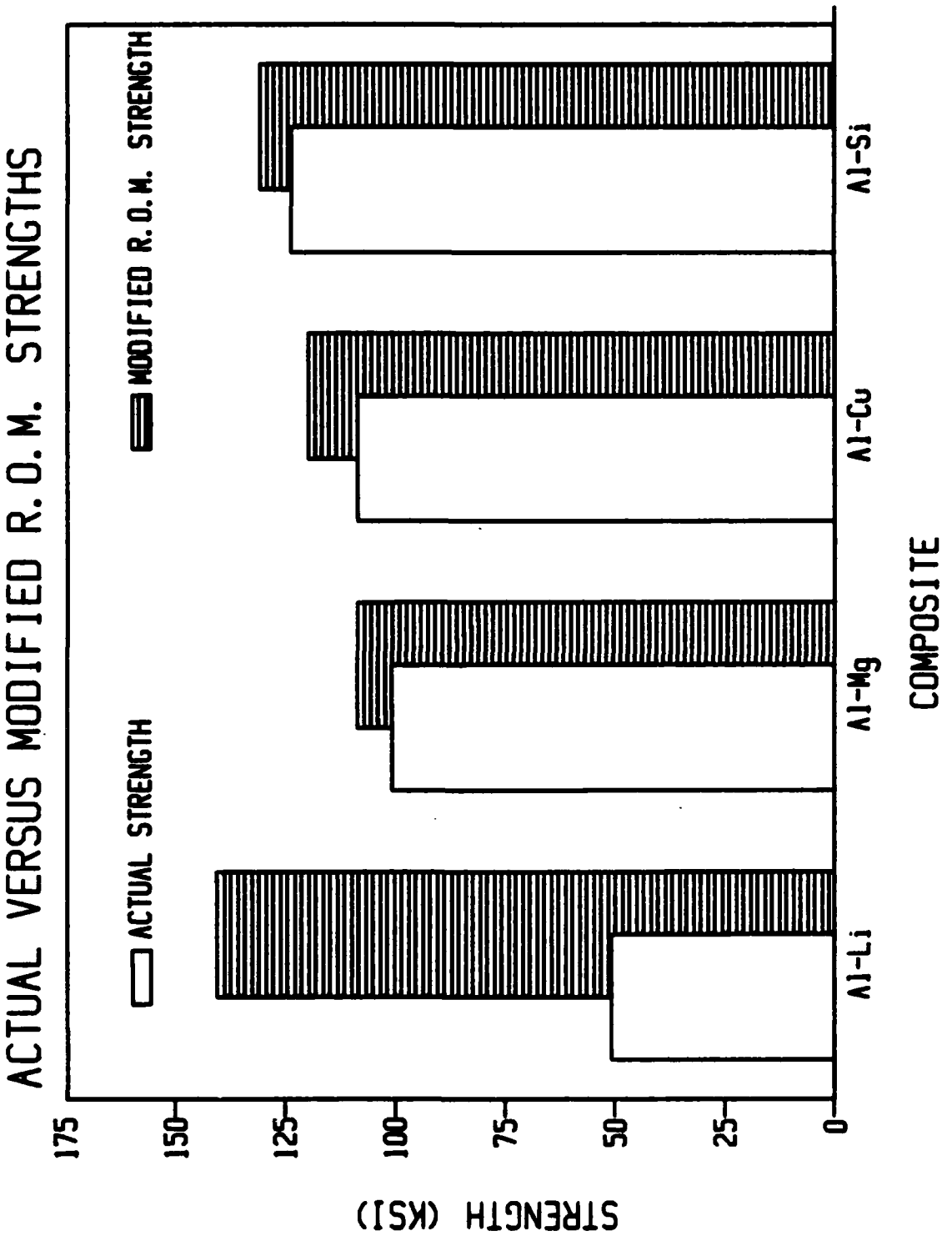

Figure 50. Actual vs. modified ROM strength for composites produced from alloy matrices

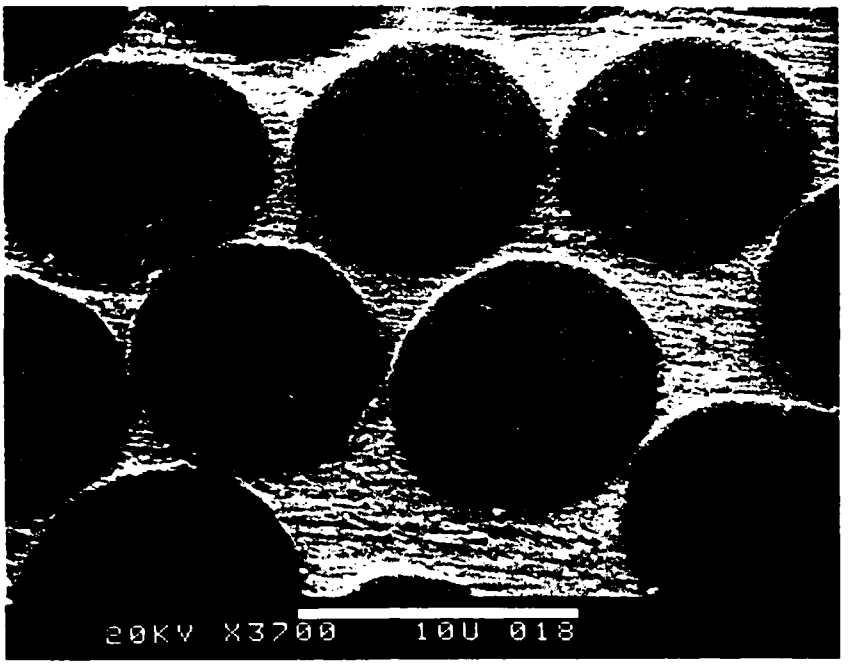

Figure 51. Typical microstructure of alloy matrix composites

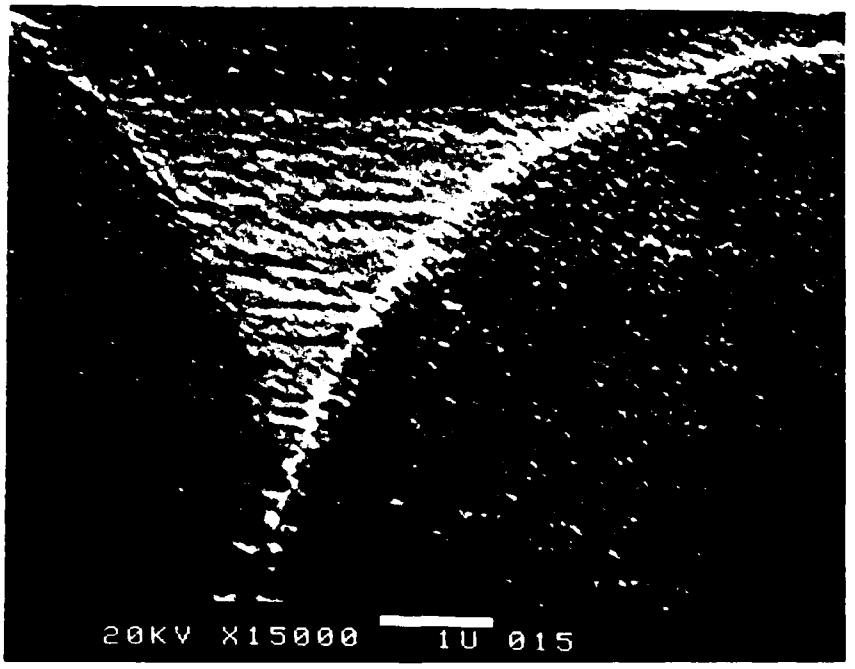

Figure 52. Typical microstructure of alloy matrix composites

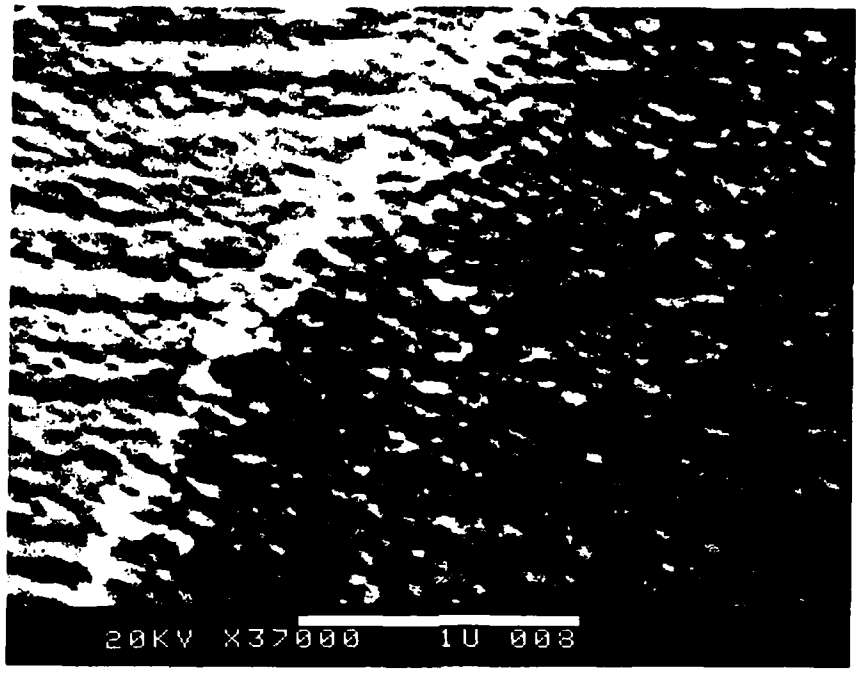

Figure 53. Typical microstructure of alloy matrix composites

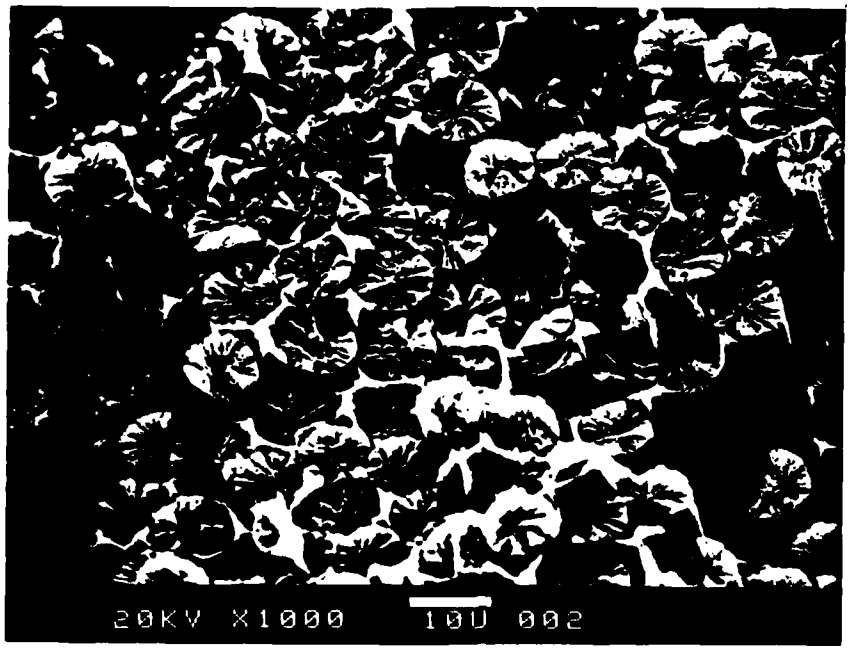

Figure 54. Typical longitudinal composite fracture surface

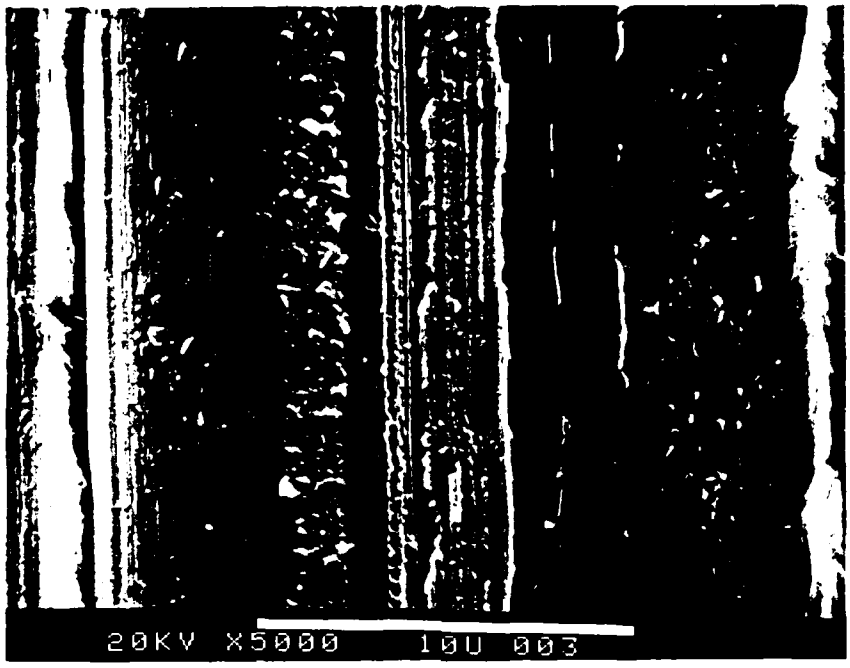

Figure 55. Transverse fracture surface from Al-Si matrix composite

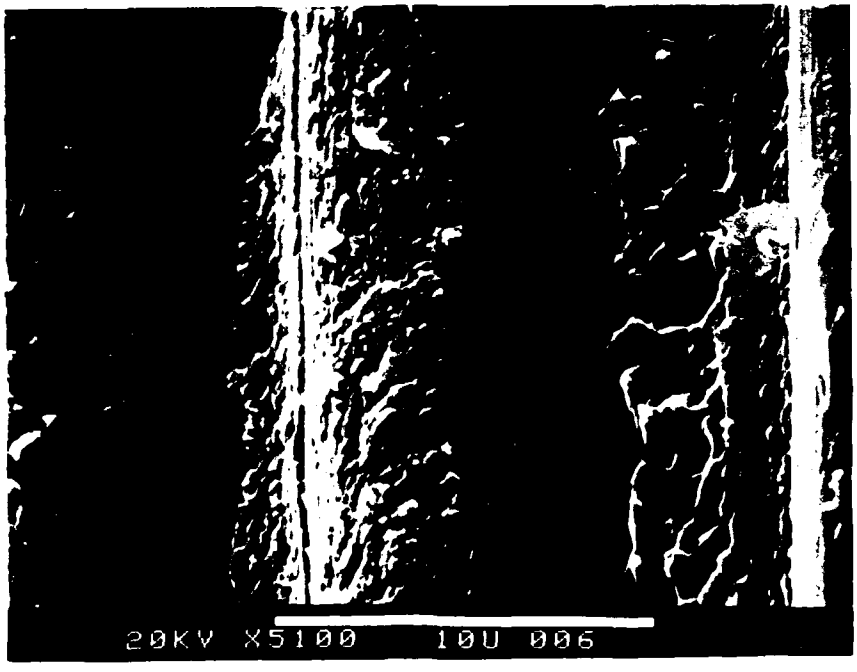

Figure 56. Transverse fracture surface from Al-Mg matrix composite

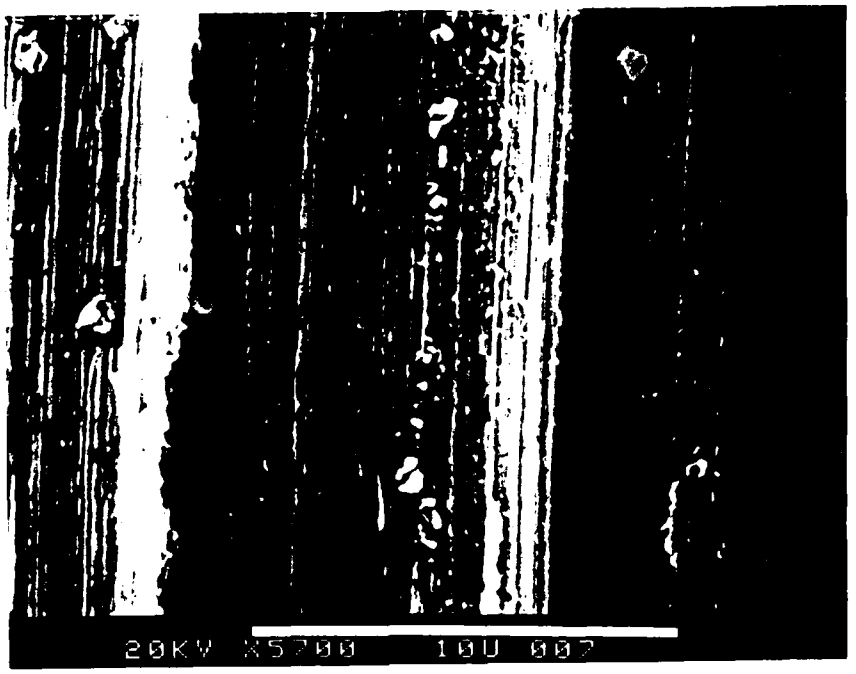

Figure 57. Transverse fracture surface from Al-Li matrix composite

Figure 58. Transverse fracture surface from Al-Cu matrix composite

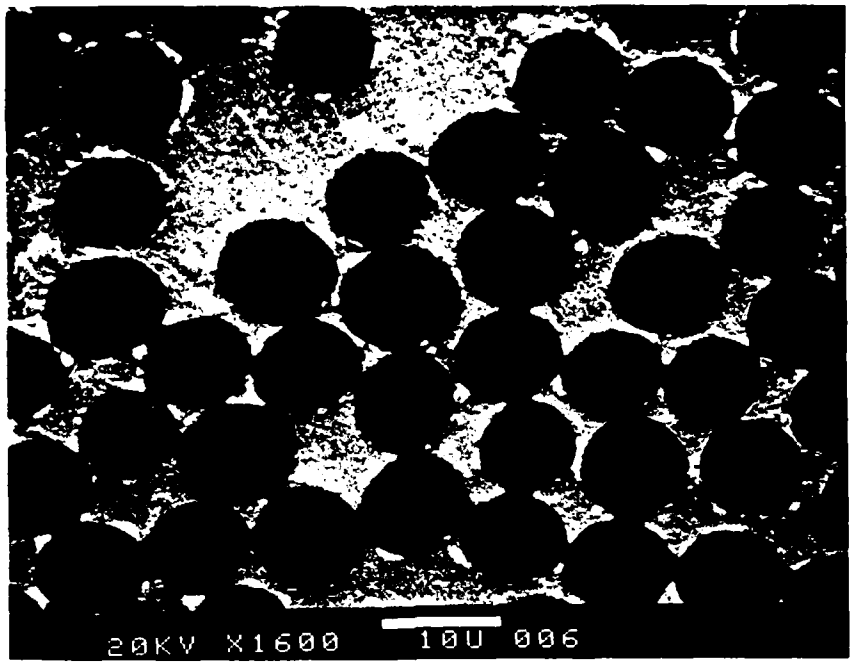

Figure 59. Microstructure of Al-Cu matrix composite showing $CuAl_2$ at the interface

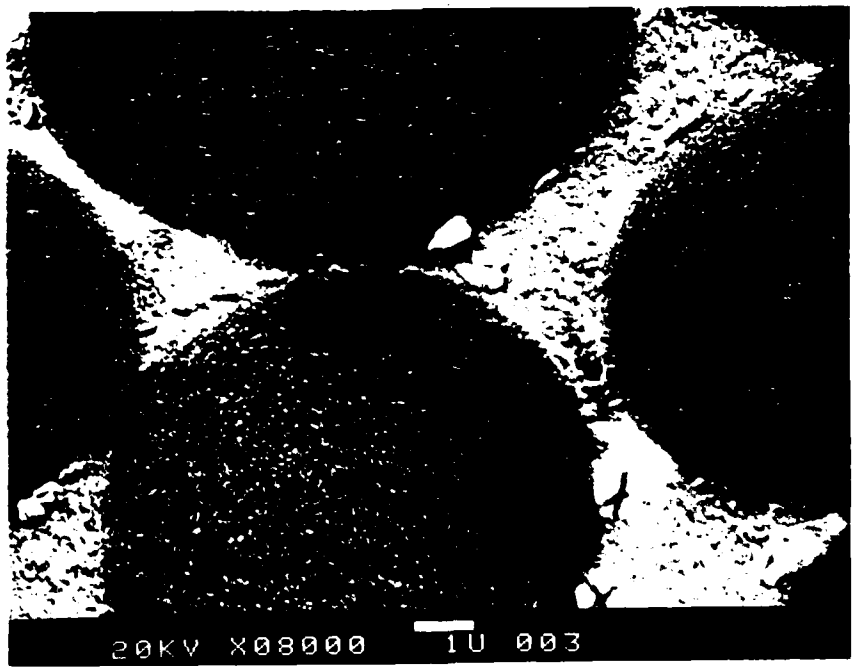

Figure 60. Microstructure of Al-Cu matrix composite showing $CuAl_2$ at the interface

Figure 61. Micrograph of Al-Si alloy showing second phase at the interface (600x)

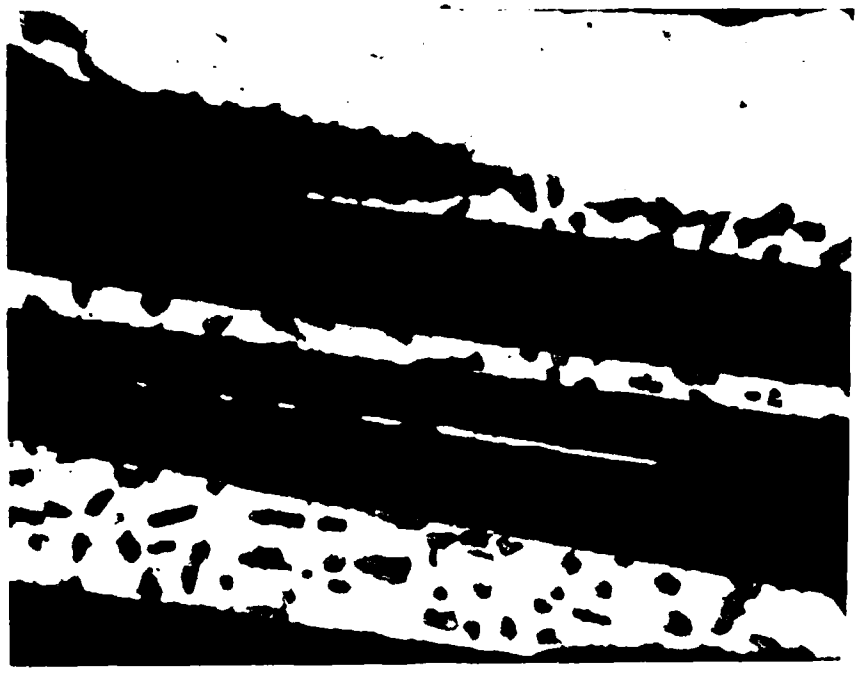

Figure 62. Micrograph of Al-Si Alloy showing second phase at interface (1500x)

FIBER STRENGTH

Uncoated P55 Tape

NO.	STRENGTH (KSI)
1.	120
2.	158
3.	161
4.	191
5.	247
6.	253
7.	284
8.	292
9.	296
10.	316
11.	321
12.	322
13.	329
14.	359
15.	366
16.	373

MEAN=274
STANDARD DEVIATION=79
COEFFICIENT OF VARIATION=0.289
16 SAMPLES

Table 1.

FIBER STRENGTH

Silicon Coated P55

NO.	STRENGTH (KSI)
1.	136
2.	144
3.	151
4.	156
5.	162
6.	174
7.	181
8.	192
9.	196
10.	198
11.	206
12.	213
13.	219
14.	221
15.	221
16.	236
17.	247
18.	252
19.	253
20.	254
21.	259
22.	261
23.	261
24.	264
25.	268
26.	274
27.	275
28.	278
29.	281
30.	286
31.	293
32.	312
33.	317
34.	328
35.	331
36.	342
37.	347
38.	357
39.	361
40.	384

MEAN=252
STANDARD DEVIATION=65
COEFFICIENT OF VARIATION=0.257
40 SAMPLES

Table 2.

FIBER STRENGTH

Carbon-Silicon Coated P55

NO.	STRENGTH (KSI)
1.	129
2.	146
3.	174
4.	181
5.	196
6.	206
7.	212
8.	227
9.	231
10.	244
11.	246
12.	249
13.	252
14.	259
15.	260
16.	266
17.	271
18.	276
19.	280
20.	283
21.	284
22.	291
23.	294
24.	301
25.	306
26.	307
27.	312
28.	318
29.	327
30.	329
31.	331
32.	331
33.	335
34.	336
35.	344
36.	346
37.	356
38.	359
39.	371
40.	394
41.	412

MEAN=282
STANDARD DEVIATION=65
COEFFICIENT OF VARIATION=0.230
41 SAMPLES

Table 3.

FIBER STRENGTH

Silicon-Aluminum Coated

NO.	STRENGTH (KSI)
1.	116
2.	129
3.	132
4.	144
5.	157
6.	169
7.	193
8.	204
9.	213
10.	216
11.	223
12.	229
13.	237
14.	241
15.	241
16.	241
17.	246
18.	249
19.	252
20.	256
21.	261
22.	266
23.	271
24.	274
25.	282
26.	288
27.	293
28.	296
29.	317
30.	329
31.	354
32.	367
33.	379
34.	407

MEAN=214
STANDARD DEVIATION=94
COEFFICIENT OF VARIATION=0.44
34 SAMPLES

Table 4.

FIBER STRENGTH

Carbon-Silicon-Aluminum Coated P55

NO.	STRENGTH (KSI)
1.	140
2.	147
3.	164
4.	193
5.	206
6.	213
7.	229
8.	234
9.	235
10.	239
11.	242
12.	247
13.	247
14.	249
15.	251
16.	259
17.	263
18.	268
19.	274
20.	275
21.	279
22.	283
23.	286
24.	290
25.	291
26.	294
27.	295
28.	297
29.	299
30.	303
31.	312
32.	314
33.	327
34.	333
35.	341
36.	344
37.	351
38.	355
39.	371
40.	386
41.	404

MEAN=276
STANDARD DEVIATION=60
COEFFICIENT OF VARIATION=0.218
41 SAMPLES

Table 5.

CASTING CONDITIONS

Coated Fibers-Pure Al Matrix

Specimen	Pressure	Vacuum
Uncoated P55	1200 psi	Excellent
Si-Al Coated	450 psi	Excellent
C-Si-Al Coated	450 psi	Excellent
Si-Al Coated	1000 psi	Excellent
C-Si Coated	1000 psi	Excellent

Table 6.

COMPOSITE STRENGTH

Coated Fibers-Pure Al Matrix
30% Fibers

Specimen	Average Strength	%ROM
Uncoated P55	67.7 ksi	80
C-Si Coated	58.0 ksi	62
Si-Al Coated	53.3 ksi	73
C-Si-Al Coated	47.9 ksi	57
Si Coated	40.1 ksi	47

Table 7.

CASTING CONDITIONS

SPECIMEN	PRESSURE (PSI)	VACUUM
Al-Mg	1800	EXCELLENT
Al-Si	200	EXCELLENT
Al-Cu	2000	EXCELLENT
Al-Li	2200	EXCELLENT

Table 8.

LONGITUDINAL COMPOSITE STRENGTHS

SPECIMEN	STRENGTH (KSI)	VOL.% FIBERS	R.O.M. STRENGTH (KSI)	% R.O.M.	MODIFIED R.O.M. (KSI)	% MODIFIED R.O.M.
Al-Li	51	51.2	41	36	N/A	N/A
Al-Mg	101	45.2	134	75	109	93
Al-Cu	109	42.9	135	81	120	91
Al-Si	124	49.3	133	93	131	95

Table 9.

TRANSVERSE STRENGTHS

SPECIMEN	STRENGTH (KSI)	VOL.% FIBERS
Al-Li	2.0	51.2
Al-Mg	6.1	45.2
Al-Cu	5.3	42.9
Al-Si	3.3	49.3

Table 10.

FIBER STRENGTH

P55 AS RECIEVED FROM UNION CARBIDE

NO.	STRENGTH (KSI)
1.	148
2.	166
3.	170
4.	189
5.	194
6.	206
7.	217
8.	219
9.	221
10.	222
11.	228
12.	237
13.	242
14.	242
15.	244
16.	248
17.	249
18.	251
19.	256
20.	259
21.	267
22.	271
23.	275
24.	277
25.	278
26.	281
27.	284
28.	288
29.	297
30.	301
31.	312
32.	315
33.	320
34.	326
35.	328

MEAN=246.5
STANDARD DEVIATION=58.4
COEFFICIENT OF VARIATION=0.237
35 SAMPLES

Table 11.

FIBER STRENGTH

P55 LEACHED FROM Al-Si MATRIX

NO.	STRENGTH (KSI)
1.	144
2.	148
3.	156
4.	169
5.	174
6.	183
7.	197
8.	206
9.	211
10.	213
11.	217
12.	226
13.	229
14.	232
15.	236
16.	238
17.	241
18.	242
19.	246
20.	247
21.	248
22.	252
23.	256
24.	262
25.	262
26.	263
27.	271
28.	274
29.	282
30.	288
31.	290
32.	293
33.	307
34.	316
35.	317
36.	318

MEAN=242.7
STANDARD DEVIATION=48.9
COEFFICIENT OF VARIATION=0.202
37 SAMPLES

Table 12.

FIBER STRENGTH

P55 LEACHED FROM Al-Cu MATRIX

NO.	STRENGTH (KSI)
1.	98
2.	147
3.	171
4.	189
5.	192
6.	203
7.	210
8.	212
9.	215
10.	217
11.	218
12.	223
13.	228
14.	229
15.	232
16.	238
17.	244
18.	248
19.	249
20.	252
21.	254
22.	254
23.	258
24.	260
25.	262
26.	263
27.	266
28.	269
29.	274
30.	288
31.	294
32.	302
33.	310
34.	311
35.	314
36.	319
37.	322

MEAN=217.2
STANDARD DEVIATION=68.9
COEFFICIENT OF VARIATION=0.317
37 SAMPLES

Table 13.

FIBER STRENGTH

P55 LEACHED FROM Al-Mg MATRIX

NO.	STRENGTH (KSI)
1.	97
2.	134
3.	136
4.	141
5.	144
6.	149
7.	151
8.	159
9.	163
10.	167
11.	182
12.	183
13.	189
14.	199
15.	219
16.	224
17.	225
18.	228
19.	229
20.	230
21.	232
22.	235
23.	237
24.	239
25.	240
26.	244
27.	245
28.	245
29.	251
30.	256
31.	272
32.	284
33.	290
34.	311

MEAN=203.8
STANDARD DEVIATION=60.4
COEFFICIENT OF VARIATION=0.296
34 SAMPLES

Table 14.

SUMMARY OF LEACHED FIBER STRENGTHS

Fibers Leached From Alloy Matrices

Alloy Fibers Leached From	Strength
Al-Cu	217 ksi
Al-Mg	204 ksi
Al-Si	243 ksi
Al-Li	N/A

Table 15.

APPENDIX A

A SIMPLE MICROMECHANICAL MODEL OF THE INTERFACE

ANALYSIS OF STRENGTH OF COATED FIBERS FROM FUNDAMENTAL MECHANICS CONSIDERATIONS

On perhaps the most basic level, an analysis if fiber/interface properties for strength enhancement is considered. From fundamental fracture mechanics, one can calculate the tensile stress, $\sigma_{\theta\theta}$, across an interface due to the stress field surrounding a crack tip (figure A1).

The governing equation is:

$$\sigma_{\theta\theta} = \frac{K_I}{\sqrt{2\pi r}} \left[\frac{3}{4}\cos\frac{\theta}{2} + \frac{1}{4}\cos\frac{3\theta}{2}\right]$$

The crack will propagate into the fiber at the point where $\sigma_{\theta\theta}$ becomes equal to the fiber strength σ_f for $\theta = 0$. Thus,

$$\sigma_{\theta\theta}(0) = \frac{K_I}{\sqrt{2\pi r}} = \sigma_f \tag{1}$$

Similarly, the crack will propagate along the interface when $\sigma_{\theta\theta}$ becomes equal to the interfacial cohesive strength, σ_{int} and $\theta=\pi/2$

Thus,

$$\sigma_{\theta\theta}(\pi/2) = \frac{K_I}{\sqrt{2\pi r}} \frac{\sqrt{2}}{4} = \sigma_{int} \tag{2}$$

Assuming, to a first approximation, that the elastic properties of the coating and the interface are equal and

AD-A165 992 MICROSTRUCTURE/PROPERTY RELATIONSHIPS FOR CARBON FIBER 2/2
REINFORCED ALUMINU (U) MASSACHUSETTS INST OF TECH
CAMBRIDGE MATERIALS PROCESSING CEN R G DIXON ET AL.
UNCLASSIFIED 25 JUL 85 N00014-83-K-0677 F/G 11/6 NL

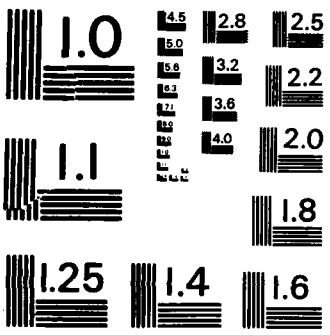

MICROCOPY RESOLUTION TEST CHART
NATIONAL BUREAU OF STANDARDS - 1963 - A

dividing Equation (1) by Equation (2):

$$R = \frac{\sigma_{int}}{\sigma_f} = \sqrt{2}/4 \tag{3}$$

Thus, if $R > 0.35$, the crack will enter the fiber and cause failure.

And, if $R < 0.35$, the crack will be diverted along the interface and the fiber will be protected by the delamination rendering the crack harmless to the fiber.

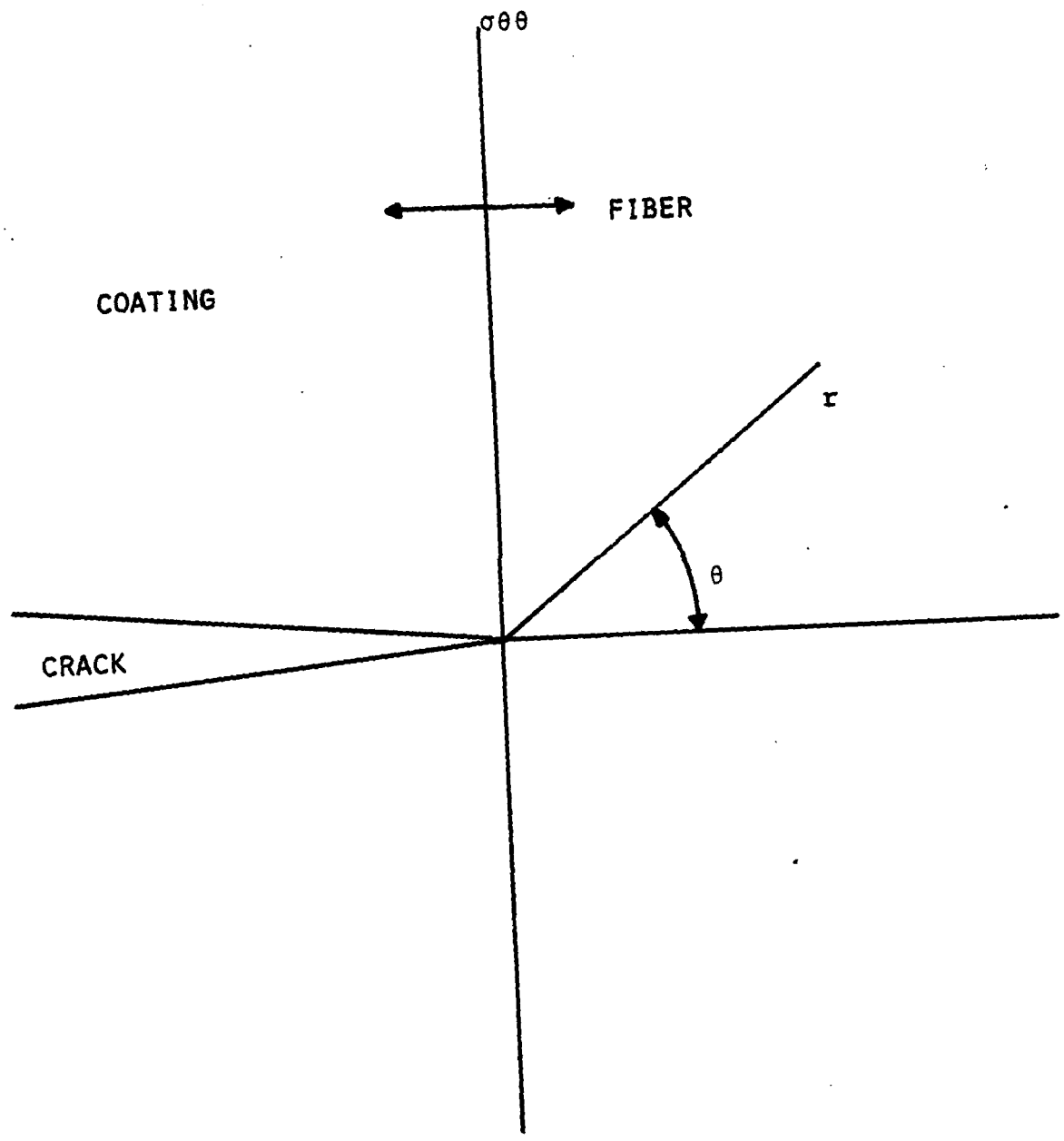

Figure 1A

APPENDIX B

EQUILIBRIUM PHASE DIAGRAMS FOR ALLOYS USED IN THIS STUDY

All phase diagrams taken from ASM Metals Handbook Volume 8, Eighth Ed.

Al-Cu ALUMINUM-COPPER

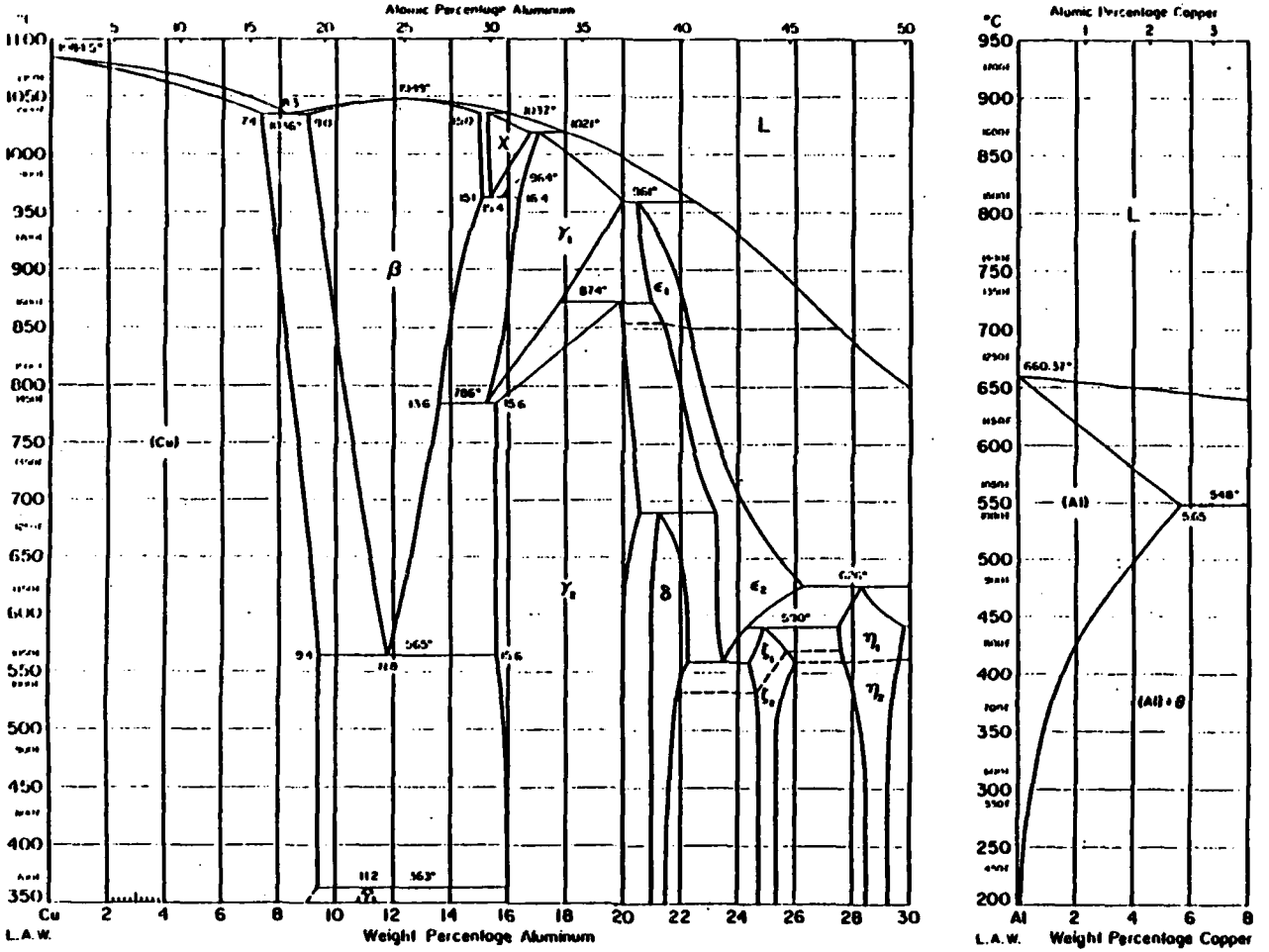

Al-Li Aluminum-Lithium

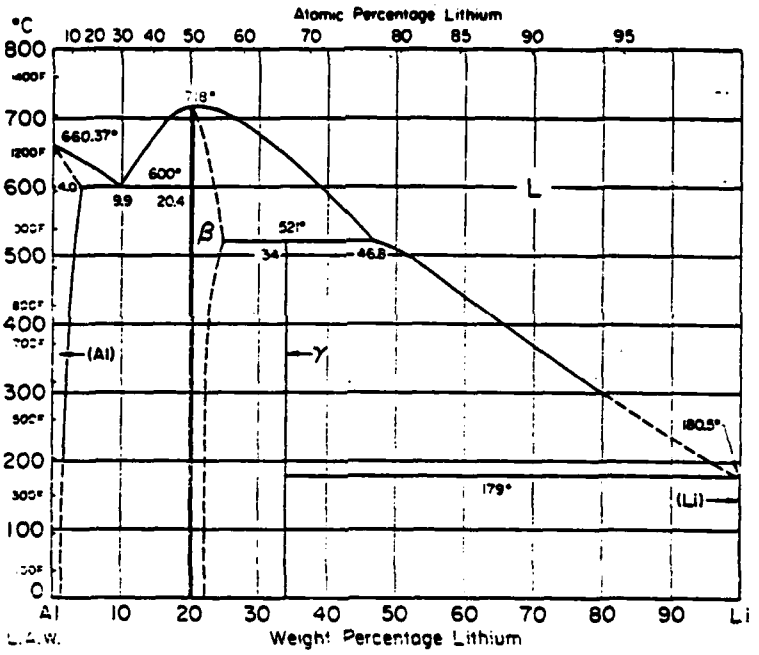

Al-Mg Aluminum-Magnesium

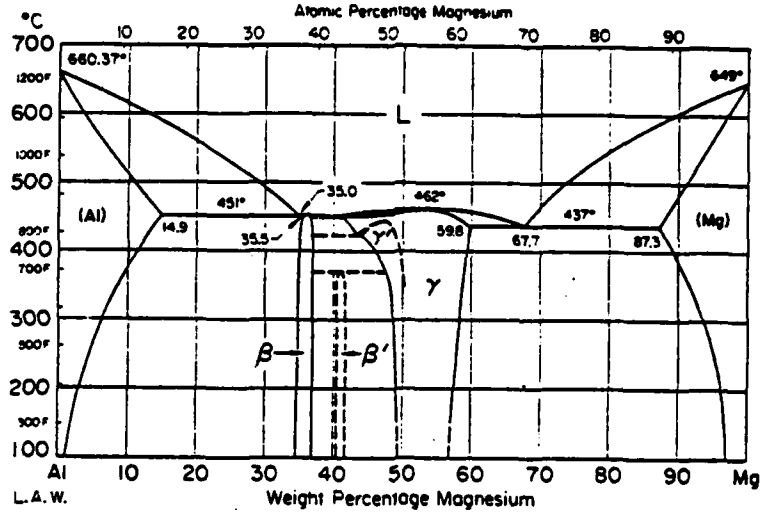

L.A.W.

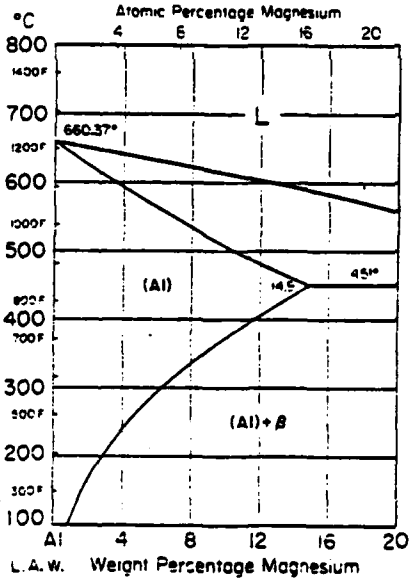

L.A.W.

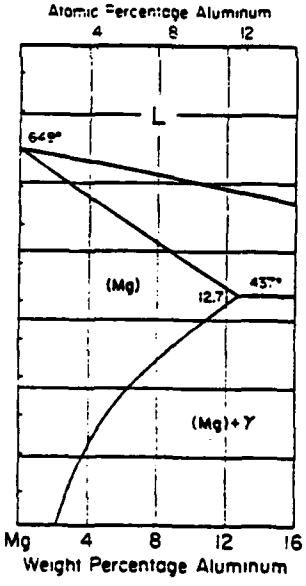

Al-Si Aluminum-Silicon

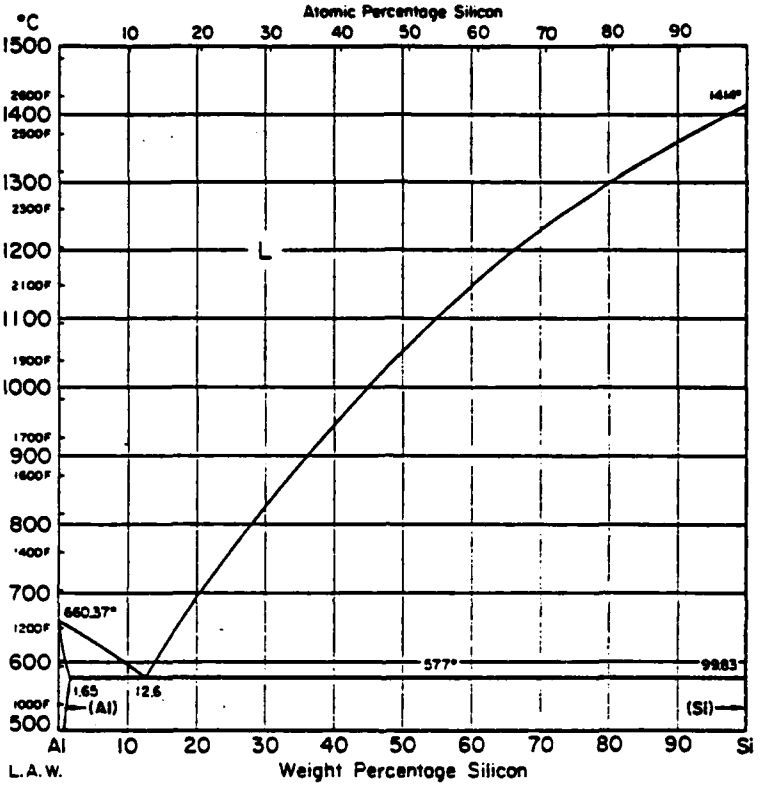

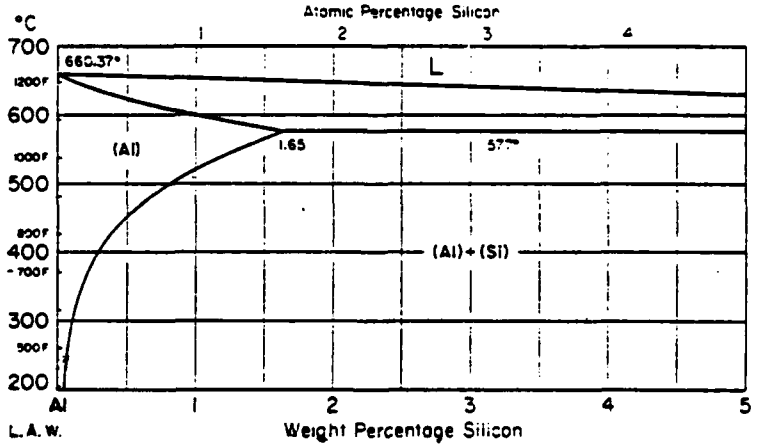

REFERENCES

1. A. Kelly, Strong Solids, Oxford Press, (1966).

2. A. A. Griffith, "The Phenomena of Rupture and Flow in Solids", Phil. Trans. Royal Society of London, A221, (1921), pp. 163-197.

3. A. A. Griffith, "The Theory of Rupture", Proc. First Int. Congress Appl. Mech., (1924), Biezeno and Burgers ed., Waltman, (1925), pp. 55-63.

4. A. Kelly, Strong Solids, Oxford Press, (1966).

5. A. Cottrell, Mechanical Properties of Matter, Wiley, (1964).

6. R. J. Diefendorf, "Carbon Fiber Structure", Proceedings--Critical Issues In Materials Technology Workshop on Transverse Strength in Carbon-Fiber/Aluminum Composites, Naval Surface Weapons Center, R. N. Lee, Ed., (April 1984), pp. 2-43 to 2-82.

7. Ibid.

8. CRC Handbook of Tables for Applied Engineering Science,2nd ed., Bolz and Tuve ed., CRC Press, (1976).

9. R. J. Diefendorf, "Carbon Fiber Structure", Proceedings--Critical Issues In Materials Technology Workshop on Transverse Strength in Carbon-Fiber/Aluminum Composites, Naval Surface Weapons Center, R. N. Lee, Ed., (April 1984), pp. 2-43 to 2-82

10. M. F. Amateau, "Progress in the Development of Graphite-Aluminum Composites Using Liquid Infiltration Technology", J. Composite Materials, vol. 10, (October 1976), pp. 279-296.

11. Ibid.

12. A. G. Metcalf and M. J. Klein, Volume 1, Interfaces in Metal Matrix Composites", Composite Materials, ed. by A. G. Metcalf, Broughtman, and Krock, Academic Press,(1974), pp. 125-168.

13. I. H. Kahn, "The Effect of Thermal Exposure on the Mechanical Properties of Aluminum-Graphite Composites", Met. Trans A, vol. 7A, (September, 1976), pp. 1281-1289.

14. Roger T. Pepper and Robert A. Penty, "Mechanical Properties of Graphite Composites Prepared by Liquid Phase Hot Pressing", J. Composite Materials, vol. 8, (January 1974), pp.29-37.

15. A. G. Metcalf and M. J. Klein, Volume 1, Interfaces in Metal Matrix Composites", Composite Materials, ed. by A. G. Metcalf, Broughtman, and Krock, Academic Press,(1974), pp. 125-168.

16. A. G. Metcalf and M. J. Klein, Volume 1, Interfaces in Metal Matrix Composites", Composite Materials, ed. by A. G. Metcalf, Broughtman, and Krock, Academic Press,(1974), pp. 125-168.

17. E. Friedrich and W. Pompe, "The Influence of Brittle Poundary Layers on the Strength of Fibrous Metallic Composites", J. Materials Sci., vol. 9, (1974), p.1911.

18. M. Shorshorov, L. M. Ustinov,and V. I. Zhammowa, "Bonding of Solid State Materials", Soviet Contribution to Working Group on Electrometallurgy, Government Committee of USSR Ministries for Science and Technology, Part I, Moscow, 1977.

19. J. A. Cornie, W. R. Lovic, and A. T. Male ,"Effect of Interface Reactions on Properties of HfC Coated SiC Fiber/Superalloy Matrix Composites",Failure Modes in Composites IV, J. Cornie and F. Crossman Ed., TMS-AIME, 1979, pp. 236-264.

20. Roger T. Pepper and Robert A. Penty, "Mechanical Properties of Graphite Composites Prepared by Liquid Phase Hot Pressing", J. Composite Materials, vol. 8, (January 1974), pp.29-37.

21. S. Ochiai and Y. Murakami, J. Mat. Sci., vol 14, (1979), pp.831-840.

22. G. Blankenburgs, "The Effect of Carbide Formation on the Mechanical Behaviour of Carbon-Aluminum Composites", The Journal of The Australian Institute of Metals, vol. 14, number 4, (November 1969), pp.236-241.

23. W. C. Harrigan, Jr., "The Effects of Temperature and Pressure on the Interface Chemistry in the Graphite-Aluminum Composite System", Met. Trans. A, vol. 9A, (April 1978), pp. 503-507.

24. Roger T. Pepper and Robert A. Penty, "Mechanical Properties of Graphite Composites Prepared by Liquid Phase Hot Pressing", J. Composite Materials, vol. 8, (January 1974), pp.29-37.

25. P. W. Jackson, "Some Studies of the Compatibility of Graphite and Other Fibers with Metal Matrixes", Metals Engineering Quarterly, (August 1969), pp. 22-30.

26. I. H. Kahn, "The Effect of Thermal Exposure on the Mechanical Properties of Aluminum-Graphite Composites", Met. Trans A, vol. 7A, (September, 1976), pp. 1281-1289.

27. Ali S. Argon, private conversation.

28. Annual Book of ASTM Standards Volume 15.03, pp. 181-187, (1984) pp. 223-231.

29. ASM Metals Handbook Volume 8, 8th ed., p. 124.

30. K. E. Cooper, A. Zangvil, and M. Metzger, "Selective Corrosion Paths and Microstructure in a Gr/Al Composite", Proceedings--Critical Issues In Materials Technology Workshop on Transverse Strength in Carbon-Fiber/Aluminum Composites, Naval Surface Weapons Center, R. N. Lee, Ed., (April 1984), pp. 2-117 to 2-120.

31. J. Lo, D. Finello, M. Schmerling, and H. L. Marcus, "Interface Structure of Heat-Treated Aluminum-Graphite Fiber Composites",Mechanical Behavior of Metal-Matrix Composites, J. Hack and M. Amateau, Ed., TMS-AIME, (February, 1982), pp. 77-82.

32. L. Christodoulou, L. Struble, and J. Pickens, "Stress Corrosion Cracking in Al-Li Binary Alloys", Aluminum-Lithium Alloys, Sanders and Starke, Ed., TMS-AIME, (1983), pp. 561-579.

33. ASM Metals Reference Book, (1981), p. 243.

34. Ibid.

35. William F. Smith, Structure and Properties of Engineering Alloys, McGraw-Hill, (1981), p. 207.

36. Andreas Mortensen, private communication.

37. Mehmet Gungor, private communication.

END

DTIC

5-86